micromachines

MDPI

Review

Mechanisms and Materials of Flexible and Stretchable Skin Sensors

Yicong Zhao and Xian Huang *

Biomedical Engineering, School of Precision Instrument and Opto-Electronics Engineering, Tianjin University, Tianjin 300072, China; zhaoyicong@tju.edu.cn

* Correspondence: huangxian@tju.edu.cn; Tel.: +86-22-2740-9253

Academic Editors: Seung Hwan Ko, Daeho Lee and Zhigang Wu

Received: 9 January 2017; Accepted: 21 February 2017; Published: 28 February 2017

Abstract: Wearable technology has attracted significant public attention and has generated huge societal and economic impact, leading to changes of both personal lifestyles and formats of healthcare. An important type of devices in wearable technology is flexible and stretchable skin sensors used primarily for biophysiological signal sensing and biomolecule analysis on skin. These sensors offer mechanical compatibility to human skin and maximum compliance to skin morphology and motion, demonstrating great potential as promising alternatives to current wearable electronic devices based on rigid substrates and packages. The mechanisms behind the design and applications of these sensors are numerous, involving profound knowledge about the physical and chemical properties of the sensors and the skin. The corresponding materials are diverse, featuring thin elastic films and unique stretchable structures based on traditional hard or ductile materials. In addition, the fabrication techniques that range from complementary metal-oxide semiconductor (CMOS) fabrication to innovative additive manufacturing have led to various sensor formats. This paper reviews mechanisms, materials, fabrication techniques, and representative applications of flexible and stretchable skin sensors, and provides perspective of future trends of the sensors in improving biomedical sensing, human machine interfacing, and quality of life.

Keywords: flexible electronics; stretchable electronics; skin sensors; precision medicine; health monitoring; wearable technology

1. Introduction

Rapid growth in electronic technology yields miniaturized electronic devices and recent evolution of wearable electronic technology that can be integrated on human bodies and conduct diverse functions, such as mobile computation [1], health monitoring [2,3], activity tracking [4–6], and rehabilitation [7]. Wearable electronic devices can combine with portable electronic gadgets such as cell phones, laptops, and tablets to offer access to remote resources and enable data exchange, analysis and diagnosis. The wearable devices demonstrated both by various commercial available devices [8] as well as devices under exploration [9] have shown great promise to enrich personal health records and facilitate biomedical informatics, both of which are considered essential elements in the newly proposed precision medicine [10,11]. However, current wearable devices are predominately realized by encapsulating integrated circuits on solid substrates in rigid packages, which are mechanically incompatible with soft and curvilinear human body, resulting in unreliable and unrepeatable measurement results due to unreliable skin contact and changing measurement locations.

Some wearable devices are based on flexible and stretchable skin sensors, which are used primarily for biophysiological signal sensing and biomolecule analyzing on skin. These sensors can serve as activity tracking devices to record basic biophysiological parameters, or used for facilitating diagnosis and treatment of certain diseases such as diabetes [12], cystic fibrosis [13], dermatitis [14,15], and

peripheral vascular disease [16]. In addition, they can be used as human–computer interface to assist human with speech and action disorders [17,18]. Additional use of skin sensors may involve monitoring exogenous parameters such as air qualities, environmental temperature, ultraviolet (UV) exposure, and humidity, allowing comprehensive assessment of health-related issues by considering both environmental and internal effects. The skin sensors offer mechanical compatibility to human skin and maximum compliance to skin morphology and motion. Stretchability is essential for these skin sensors, as the sensing precision, repeatability, stability and adhesion to skin are all determined by the capability of the sensors in following the skin motion, which causes skin deformation up to 30% [19]. The skin sensors contain unique structures constructed by either intrinsically soft materials or thin film materials on elastomer substrates. They can be simply mounted on bodies using fixtures such as bandages and body straps or use improved approaches that allow spontaneous skin attachment by van der Waals force using ultrathin and soft materials [14,18,20]. In addition, pressure sensitive silicon adhesive [21,22] can also be used to enhance the interface between the sensors and the skin, and offer reversible adhesion for long-term skin integration. Although the underlying mechanisms and relevant techniques of the skin sensors have been studied in many research papers that focus on various aspects [20,23,24], it will be beneficial if a systematic summary can be offered with comprehensive review of the state-of-the-art technology in flexible and stretchable skin sensor development.

This paper reviews some essential elements of flexible and stretchable skin sensors, including their mechanisms, materials, fabrication techniques, and applications, all of which represent recent progress in both theoretical and applied research of skin sensors. The fundamental mechanisms that determine the stretchability of the sensors are first presented, followed by materials used in skin sensors and their processing techniques. Finally, representative applications of the skin sensors are presented to demonstrate their capability in the areas of biomedical sensing and daily activity tracking. Flexible and stretchable skin sensors hold the promise to replace current wearable sensors based on rigid substrates and packages, and may eventually lead to the revolutionary changes in the formats of continuous, long-term health monitoring devices to improve social health levels.

2. Mechanisms of Flexible and Stretchable Skin Sensors

Flexible and stretchable skin sensors offer maximum compliance to the skin, and, thus, minimum reaction force from the sensor in response to the deformation, allowing less influence to the normal functions of the skin. The stretchability of the skin sensors can be achieved at the structural and material levels. The former refers to unique designed structures that offer tolerance to certain levels of deformation within the limits of the fracture strain of the constituent materials, while the latter can be attributed to intrinsically soft materials that are mechanically elastic to allow reversible extension and compression in response to external forces. The following section summarizes details of these two approaches.

2.1. Stretchable Structures

Materials used in skin sensors follow a simply rule that the bending strain of the materials decreases linearly with thickness of materials [23]. As a result, composition materials of skin sensors such as semiconductors, polymers, and metals are used in formats of ribbons, wires, and membranes with thickness in the scale of tens of nanometers to a few micrometers. They can be readily bended to reach a radius of curvature of ~150 mm with ~0.1% strains [25,26], which is less than the facture strain of these materials [26]. Two design approaches have been developed to make intrinsically rigid materials stretchable on elastomeric substrates. The former design uses out-of-plane buckling of ultra-thin nanoscale wires, ribbons, or membranes to release stress caused by in-plane prestrain applied to the substrates. The latter uses stretchable interconnects as bridges to connect with rigid islands, which typically contain functional components such as sensors [27,28], electronics [29–31], and commercial off-the-shelf components [32]. Both of these strategies have been widely used in layout of stretchable skin sensors.

2.1.1. Out-of-Plane Design

The formation of out-of-plane design with buckling structure is illustrated in Figure 1a. The ultrathin ribbons can be fabricated using conventional lithography process, followed by bonding the nanoribbons on to a prestrained elastomeric substrate. Releasing of the prestrain leads to periodical wavy structures on both ribbons and the substrate. The wavelength (λ) and magnitude (A) of the wavy structures can be determined by following equation.

$$\lambda = 2\pi h_f \left(\frac{\overline{E}_f}{3\overline{E}_s} \right)^{1/3}, A = h_f \sqrt{\frac{\varepsilon_{pre} - \varepsilon_{applied}}{\varepsilon_c} - 1} \quad (1)$$

in which h_f is the thickness of the stiff ribbons, $\overline{E_f}$ the Young's modulus of the elastic substrate, $\varepsilon_{applied}$ the applied strain, ε_{pre} the prestrain level, and ε_c the critical strain for the buckled ribbons. The peak strain in the ribbon is approximately equal to

$$\varepsilon_{peak} \approx 2\sqrt{\left(\varepsilon_{pre} - \varepsilon_{applied}\right)\varepsilon_c} \quad (2)$$

As a result, the maximum stretchability of the wavy structures can be determined by equating ε_{peak} to facture strain of the ribbon materials.

Recent development of wavy design has led to more complicated three-dimensional (3D) structures that buckle at higher orders, indicating potential applications of these technologies to form miniaturized flexible and stretchable electronics with highly spatial complexity and capability to achieve predefined shape shifting and function alternation [33]. The wavy design has been wildly available to integrate silicon [24], carbon nanotubes [34–36], graphene [37] and ferroelectrics [38] in formats of nanoribbons (Figure 1b) [24], nanowires (Figure 1c,e) [39], and nanomembranes (Figure 1d) [40]. However, the stretchability of the wavy design is determined by the prestrain levels of the substrates and the bending curvature of the materials as shown in Equations (1) and (2), limiting the applications of this technology in situations that require larger stretchability and less complex fabrication processes. As a result, island–bridge configurations have been developed to offer improved stretchability with both out-of-plane and in-plane structures in which islands based on functional sensing and circuit elements are mechanically and electrically connected with bridges made of narrow polymeric and metallic strips. The bridges, which contain either straight or serpentine interconnects, are freely suspended or bond on substrates between two islands. The stretchability of such structures are achieved either by deformation of the spatially buckled bridges (Figure 2a) or planar deformation of the interconnects (Figure 3c).

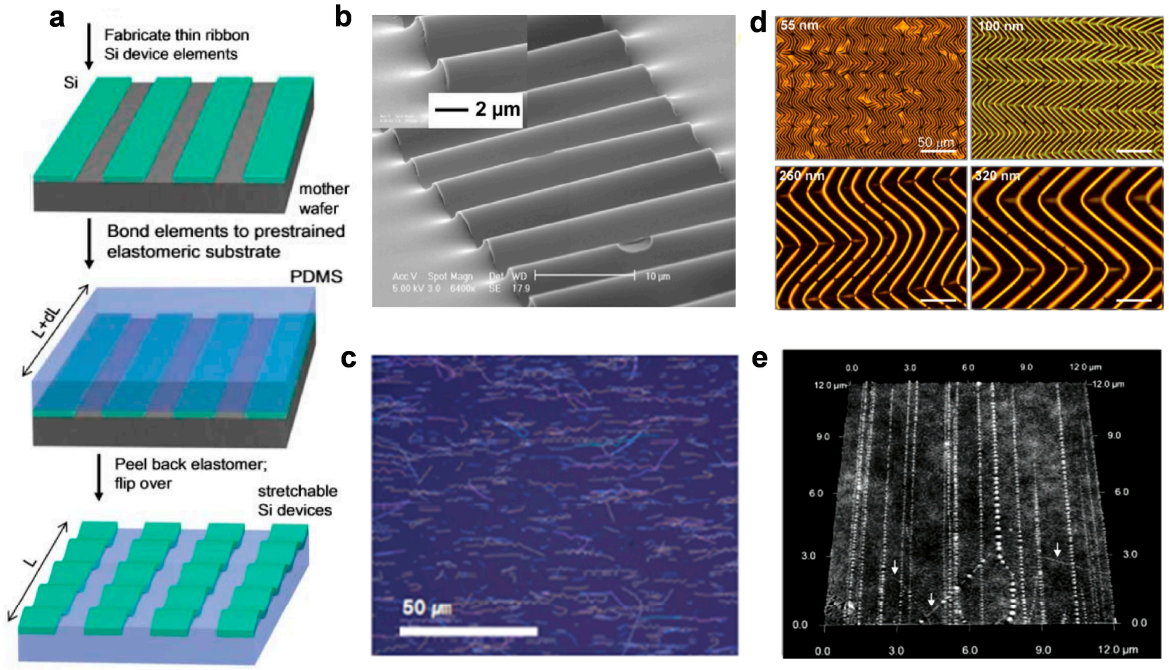

Figure 1. Mechanism of out-of-plane stretchable structures: (**a**) formation of out-of-plane nanoribbons (Reprinted with permission from Ref. [30] Copyright 2006 American Association for the Advancement of Science); (**b**) scanning electron microscope (SEM) images of a wavy nanoribbon (Reprinted with permission from Ref. [24] Copyright 2010 American Association for the Advancement of Science); (**c**) a large area optical micrograph of silicon nanowires (Reprinted with permission from Ref. [39] Copyright 2009 American Chemical Society); (**d**) optical micrographs of 2D wavy Si nanomembranes with various thickness (55, 100, 260, 320 nm) on polydimethylsiloxane (PDMS), formed with a thermal prestrain of 3.8% (Reprinted with permission from Ref. [40] Copyright 2007, American Chemical Society); and (**e**) an atomic force microscopic image of wavy SWNTs on a PDMS substrate (Reprinted with permission from Ref. [34] Copyright 2008 American Chemical Society).

Novel substrate-free spatial helical structures have also been developed using diverse twisting modes, and have been used to act as sensors and power harvesters. Shang et al. have explored a carbon nanotube (CNT) yarn supercapacitor utilizing the helical loop structure. The entire structure can withstand strain of ~150% and repeated high frequency stretching (up to 10 Hz over 10,000 cycles). A helical spring based on copper nanowire [41], as shown in Figure 2b, offers higher stretchability (~700%). Similar structures can be formed by other metallic nanowires, showing variety of potential applications in wearable sensors and interconnects that can deform with the gradual growth of body parts.

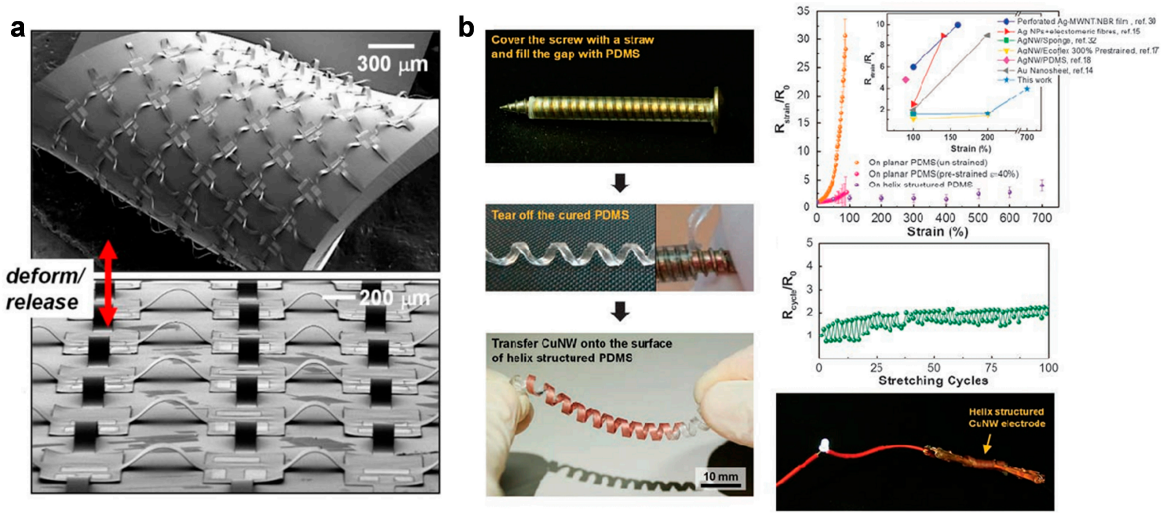

Figure 2. Examples of out-of-plane strcutres with high stretchability: (**a**) SEM images of arrays of complementary metal-oxide semiconductor (CMOS) inverters with spatially buckled bridges (Reprinted with permission from Ref. [29] Copyright 2008 National Academy of Sciences); and (**b**) helical-structured copper nanowire (CuNW)-based electrodes (Reprinted with permission from Ref. [41] Copyright 2014 Nature Publishing Group).

2.1.2. In-Plane Design

Improved deign without using prestrained substrates can be achieved by in-plane island–bridge design. The polymeric and metallic interconnects are typically in forms of serpentine or fractal [42–46] meshes that are completely bonded onto elastomeric substrates. In some cases, the island structures can be further omitted, resulting in continuous self-similar serpentine or fractal structures as both sensors and interconnects. Compared to wavy structures, these planar serpentine or fractal design effectively accommodate much larger applied strain through in-plane structural deformation without requirement of prestrain on substrates, and eliminate the concern of delicate spatially-buckled structures that can be easily broken under external scratch.

However, design of serpentine interconnect is still largely empirical, only a few theoretical models have been developed to analyze the deformation and stretchability of serpentine geometry. Fan et al. formulated an analytic model of in-planar serpentine interconnects based on finite deformation theory [47]. As illustrated in Figure 3a, a serpentine interconnect is simplified as three straight wires with length L or $L/2$ connected with two arcs with an identical radius R and an arc angle α. Three dimensionless parameters, width/radius ratio $\overline{w} = w/R$, arm length/radius ratio $\overline{L} = L/R$ and arc angle α, can then be used to represent the shape of the serpentine interconnect. As $\overline{w}$ of the non-buckled interconnect is usually much smaller than 0.5, such interconnect can be modeled as a curved, Euler–Bernoulli beam. When the serpentine interconnect is subjected to a tensile displacement of $U_{\text{app}}/2$ at the end, the effective applied strain ε_{app} of the serpentine interconnect can be represented by

$$\varepsilon_{\text{app}} = \frac{U_{\text{app}}}{4R\sin(\alpha/2) + 2L\cos(\alpha/2)} \tag{3}$$

The peak value of maximum principal strain in the serpentine interconnect can be related to the applied strain and the geometric parameters by

$$\varepsilon_{\text{max-nonlinear}} = \overline{w}F_2\left(\overline{L}, \alpha, \varepsilon_{\text{app}}\right) \tag{4}$$

where $F_2\left(\overline{L}, \alpha, \varepsilon_{\text{app}}\right)$ is a function that can be determined numerically using an approximate model based on finite deformation theory.

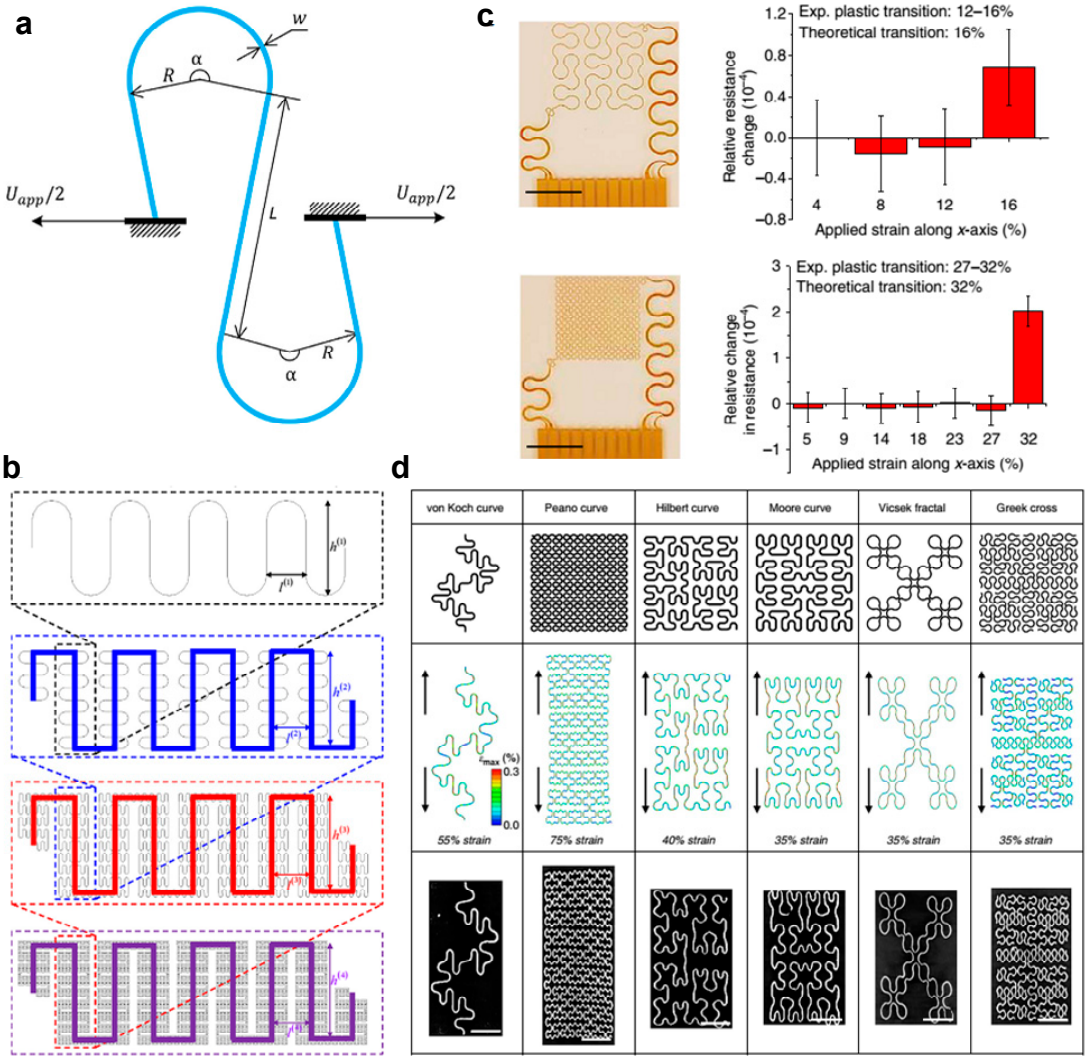

Figure 3. Mechanisms of serpentine and fractal structures: (**a**) a serpentine interconnect subjected to an axial stretching (U_{app}) at the two ends (Reprinted with permission from Ref. [47] Copyright 2016 Elsevier); (**b**) schematic illustration on the geometric construction of self-similar serpentine interconnects (Reprinted with permission from Ref. [48] Copyright 2013 Elsevier); and (**c**,**d**) representatives of fractal structures (Reprinted with permission from Ref. [45] Copyright 2014 Nature Publishing Group).

A fractal design concept that allows formation of stretchable layouts through stepwise iterations of basic shape units has been introduced to realize highly stretchable lithium-ion batteries [43] as well as several epidermal sensors [31,44,49]. As illustrated in Figure 3b, a fractal-based layout is created from the first order of serpentine geometry, and then constructed by connecting multiple copies of the unit cell forming self-similar design that offers increased area coverage and improved stretchability [48]. Theoretical models have been developed to analyze the deformation and stretchability of the fractal geometry. Fan et al. [45] have studied the deformations of various fractal layouts (Figure 3d), using a finite element method (FEM) followed by experimental evaluation. They also introduced a high precision approach to measure the elastic-plastic transition (or the elastic stretchability) through measuring differential resistances of the fractal interconnects, showing reasonable consistency with numerical analysis (Figure 3c). Several analytical models have been developed to determine elasticity for fractal interconnects. For example, Zhang et al. [48] have developed analytical models of flexibility and elastic stretchability, through establishing recursive formulae at different fractal orders. The

analytical models show that the stretchability of system increases with the order of self-similar interconnect, and a surface filling ratios of 50% would yield 70% stretchability. In addition, the tensile stiffness for fractal interconnects has been determined by analytic approach, and has been verified by finite element analysis and experiments [50].

2.2. Intrinsic Elastic Materials

The stretchability of skin sensors can be achieved at the material levels using intrinsic elastic materials. Major materials in this category include elastomers and liquid metals, all of which adopt the stretchability due either to the flexible and long polymer chains or to weak intermolecular forces. This section offers a general review of the mechanism of these materials, while a detailed list of these materials will be given in next section.

One of the most widely used materials in stretchable skin sensors is silicone-based elastomers represented by polydimethylsiloxane (PDMS), fluorosilicone and various commercially available products under different tradenames such as Ecoflex, Dragon Skin, and Solaris. Silicone-based elastomers are notable for their high electrical resistivity (e.g., 2.9×10^{14} Ω·cm for PDMS), low glass transition temperatures (e.g., −125 °C for PDMS), large thermal coefficient of expansion (typically 4.8×10^{-4} K^{-1}) and high flexibility (with Young's module of 1 MPa). The polymer chains of the silicone contain siloxane backbones that consist of alterative sequences of silicon and oxygen and two organic substituents connected to each silicon atom, resulting in various properties (e.g., chemical resistance, elasticity, and phase) and processibility (e.g., curing time, and curing temperature). The elastomers obtain their stretchability through highly flexible siloxane backbones, which can be stretched under external forces. Another material that widely used in stretchable skin sensors is polyurethane (PU), which contains urethane groups connected with other groups such as ester, ether, amine and urea. The PU elastomers adopt their elasticity from the elastic polyol parts in the polymer chains, and offer large tear strength and abrasion resistant than silicone rubbers, making them ideal materials to construct substrates for skin sensors when frequent surface scratch and impact are expected.

3. Materials in Skin Sensors

The major materials of stretchable skin sensors can be classified into two categories. One involves various intrinsically stretchable materials, such as elastomers, liquid metals, and composite materials. The other includes materials such as solid metals, semiconductors, polymers, and inorganic compounds, which are rigid as bulk materials, but can be used as ultrathin films or membranes designed into special stretchable structures with thickness ranging from tens of nanometers to tens of micrometers. Therefore, the Young's modulus of the materials for stretchable skin sensors are wildly distributed from 0 to 10^{12} Pa [51].

3.1. Physically Soft and Stretchable Materials

3.1.1. Elastomers

Elastomers are available in different compositions with varied stretchability. As the fundamental materials in stretchable skin sensors, elastomers are mainly used as substrates, binders and adhesion layers. Among the available elastomers, PDMS is most commonly used. The mechanical properties of PDMS can be tuned by varying the curing conditions such as chemical ratios, temperature, and time, resulting in a Young's modulus in a controllable range from 1 to 150 MPa, and a stretchability up to 100%. By alternating the side groups as well as the lengths of the polymer chains, it is possible to obtain different types of elastomers with different physical and chemical properties. For example, PU and acrylic elastomer are two alternatives for skin sensor substrates, and are softer than PDMS due to its low Young's modules. The maximum stretchability that can be achieved is 300% [52]. The low-temperature curing silicone is a type of adhesive that can provide pressure sensitive reversible bonding between the skin and the devices. Besides of mold casting, silicone such as PDMS and polyurethane acrylate (PUA)

can be photocurable to allow pattern definition through traditional photolithography processes [53,54] or even 3D printing techniques [55].

3.1.2. Liquid Metals

Liquid metals such as eutectic gallium-indium (eGaIn) and gallium-indium-tin (Galinstan) are intrinsically elastic with low resistivity (~2.9×10^{-7} Ω·m), low viscosity (~2×10^{-3} Pa·s), and low toxicity [56]. Their melting points are 15.5 °C [57] (75 wt % Ga and 25 wt % In) and −19 °C [58] (68.5 wt % Ga, 21.5% In, and 10.0% Sn), respectively, resulting in their liquid states at room temperature. Various functional components such as pressure sensors [59,60], strain sensors [61], antennas [62,63], and soft wires [64] have been fabricated by injecting liquid metals into microfluidic channels. Devices made of liquid metals can withstand deformation of microchannels at very high strain (up to 800%) [65].

3.1.3. Conductive Polymers

Conductive polymers (CPs) applied in stretchable electronics can be achieved by intrinsically conductive polymers (ICPs) [66] or conductive polymer composites [67]. Intrinsically conductive polymer materials such as synthetic poly(acetylene) (PA), poly(pyrrole) (PPy), poly(thiophene) (PT), poly(aniline) (PANI), and poly-(3,4-ethylenedioxythiophene) (PEDOT) can be realized by conjugation of polymer backbone, forming high energy orbitals with loosely bonded electrons to corresponding atoms, allowing maximum facture strain at the level of 1000% [68]. The conductive polymer composites are composed of polymers and conductive fillers (e.g., metal nanoparticles, metal nanowires, graphite, carbon nanotubes, and graphene). Conductive polymers are subject to influence of strain, which may lead to increased resistivity with strain. Park et al. have demonstrated a conductive composite mat using electrospun poly(styrene-block-butadiene-blocks-tyrene) (SBS) rubber fibers embedded with silver nanoparticles, leading to high conductivity even under large deformations ($\sigma \approx 2200$ S·cm^{-1} at 100% strain) [69]. Shang et al. have achieved an elastic conductive nanocomposite composed of multiwall carbon nanotubes (MWNTs) and polyurethane (PU), which has initial conductivity of more than 5.3 S·cm^{-1} and stretchability of more than 100% [70]. Niu et al. have realized buckled single-wall carbon nanotube (SWCNT) electrodes by fabricating directly grown SWCNT films with continuous reticulate architecture on pre-strained PDMS [71]. The electrodes can stretch under a strain of 140% without significant change of resistance.

3.1.4. 1D and 2D Materials

The applications of one-dimensional (1D) and two-dimensional (2D) materials to construct stretchable electronics represent important trends in constructing stretchable electronics. Representative 1D and 2D materials include multi-walled or single-walled carbon nanotubes [72,73], silicon nanowires [74], metal nanowires [75,76], graphene [77], and transition metal dichalcogenides (TMDCs) [78]. Among them, both carbon nanotubes and graphene possess high electron mobility (~10^5 cm^2·v^{-1}·s^{-1} for carbon nanotube [79] and ~2×10^5 cm^2·v^{-1}·s^{-1} for graphene [80] at room temperature) and excellent mechanical flexibility (~1 Tpa Young's modulus) [81], making them promising materials for high performance electronic devices, such as top-gated transistors [82–84]. When used as sensors, the large surface-to-volume ratios of the 1D and 2D materials can lead to improved capabilities, such as highly sensitive biochemical sensing and large interfacial adhesion [85]. In addition, the optical transparency of graphene and carbon nanotubes allows construction of fully transparent sensors that possess high flexibility and softness [86,87]. Some excellent reviews about the 1D and 2D materials used in flexible and stretchable electronics have been provided by the following articles [88–90].

3.2. Unique Stretchable Structures

As mentioned in the previous section, raw materials that are rigid in their bulky formats can also offer stretchability in ultrathin configurations and unique stretchable design. Some

major materials used for constructing skin sensors include metals, semiconductors, polymers, and inorganic compounds.

3.2.1. Solid Metals

Solid metals are intrinsically hard conductive materials that would become flexible when appear as thin films. Dominant metals used in skin sensors include Au, Cu, Al, Cr, Ti and Pt, which are used for conductive interconnects, electrodes, sensors, contact pads and other circuit components (e.g., resistor, inductors, and capacitors). These metals are typically tens of nanometers to a few micrometers in thickness, and are deposited on target substrates through physical deposition, electrochemical plating, and direct printing approaches. Many of these metals are ductile with a fracture strain of less than 1%. However, the stretchability of the metallic thin films can reach more than 100% when designed into special formats such as self-similar serpentine [91], fractal [28], helical [92] and prestrained bulking [29].

3.2.2. Semiconductors

Various active components such as diodes, transistors, and light emitting diodes (LED) can be made of inorganic semiconductor materials (e.g., silicon [30], GaAs [93], ZnO [94], InP [95], GaN [96]) as well as organic semiconductor materials (e.g., poly(3-hexylthiophene) (P3HT) [97], Poly(p-phenylene)vinylene [98], and Poly(2,5-bis(3-hexadecylthiophen-2-yl)thieno[3,2-b]thiophene) (pBTTT)) [99]. The bending stiffness and bending-induced strain of these rigid semiconductor materials can be exceptionally small due to cubic and linear scaling of these quantities with thickness of the materials. These semiconductor materials can be patterned into nanomembranes [100], nanoribbons [101], and nanowires [95] through complementary metal-oxide semiconductor (CMOS) fabrication processes.

3.2.3. Polymers

Polymers offer mechanical and electrical supports to skin sensors. They can be used as structural layers, electrical insulation layers, and dielectric layers in the skin sensors. Many polymers have been used to construct skin sensors, including some most prominent ones such as polyimide, poly(methyl methacrylate) (PMMA) and parylene. These polymers offer high mechanical strength that are ideal as structural layers to support the skin sensors. In addition, these polymers are typically thermal setting materials that can be easily obtained through spin-coating and dipping followed by curing at escalated temperature. Parylene is an excellent dielectric material, its fabrication process involves chemical vapor deposition (CVD), allowing pinhole-free uniform layers on curved or irregular surface.

4. Fabrication Techniques

Fabrication of skin sensors involve a series of techniques that combine conventional fabrication methods such as microelectromechanical systems (MEMS) technology, CMOS process, and mechanical milling with emerging techniques such as printable electronic, additive manufacturing, and laser process. Under the support from diverse fabrication techniques, many materials can be processed to yield structures in stretchable skin sensors.

4.1. Conventional Microfabrication Processes

Fabrications of active and passive components in flexible and stretchable electronic skin sensors can be achieved by MEMS and CMOS technology. The fundamental challenge of using MEMS and CMOS technology to make skin sensors involve application of ultrathin membranes as compared with rigid or brittle materials used in traditional MEMS and CMOS fabrication processes. Processes for fabricating flexible and stretchable skin sensors can be categorized into device-last and device-first approaches. The former involves fabricating active components on silicon membranes on silicon-on-insulator substrates, and then transfer-printing the membranes to destination substrates for

further processing. While the latter refers to thinning down a thick semiconductor substrates integrated with functional components using physical sanding or chemical etching methods. The device-last approaches have been described by several research works. For example, Kim et al. [26] have developed stretchable integrated circuits, which combine multilayer neutral mechanical plane layouts and "wavy" structural configurations, including logic gates, ring oscillators, and differential amplifiers on silicon nanomembrane with thickness of 250 nm (Figure 4a). The device-first approaches have been demonstrated by MOS capacitors [102,103], memory cells [104,105], batteries [106], and MEMS switches [107].

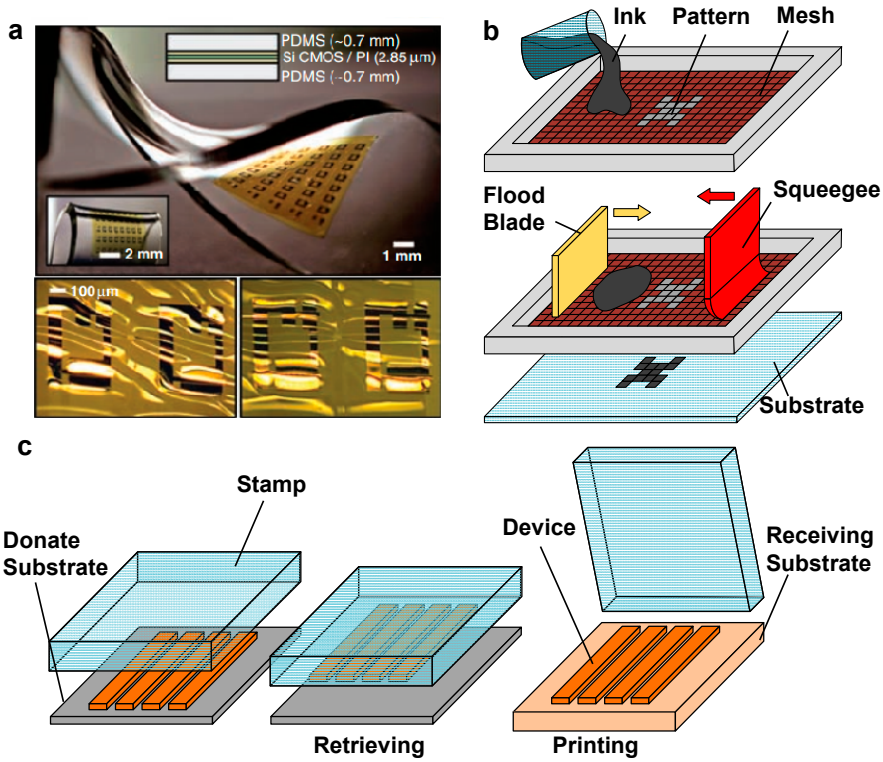

Figure 4. (**a**) Stretchable integrated circuits fabricated based on CMOS technology (Reprinted with permission from Ref. [26] Copyright 2008 American Association for the Advancement of Science); (**b**) a schematics of the screen printing process; and (**c**) a schematics of the transfer printing process.

Simplified approaches for making active and passive components involve using both organic materials as conductors, semiconductors, and dielectric to construct electronic devices. The major fabrication processes include chemical or physical vapor deposition, spin-coating and dip coating, which are much convenient than conventional microfabrication processes of inorganic materials, whose fabrications typically require thermal diffusion, ion implantation, and highly corrosive acid etchant used in inorganic materials. However, drawbacks of using organic materials are their low conductivity (1000 $S \cdot cm^{-1}$) and low charge mobility (approximately 10^{-2} to 10^{2} $cm^2 \cdot v^{-1} \cdot s^{-1}$) [108,109], which hinder the applications of organic materials in high performance electronics.

4.2. Printable Electronics

Continuous development of printing electronic technology enables the application of such technology in developing flexible and stretchable electronics. Printable electronic technology allows direct generation of patterns on soft substrates through additive manufacturing technology such as screen-printing, slot-die coating and inkjet printing. In addition, a special printing approach used primarily in flexible and stretchable electronics is based on transfer printing, which transfer

components fabricated on donate substrates onto target substrates that are typically thin plastic films, metal foils, and elastomer membranes.

4.2.1. Screen Printing

Screen printing is a low-cost, high-throughput printing technique used to construct skin sensors. The working principle of screen printing system is illustrated in Figure 4b. A screen printing system typically contains a flood blade that moves across a screen with open meshes with pore sizes ranging from 10 to 200 μm [110,111] and fills the meshes with ink. A squeegee is then moved in an opposite direction to push the inks in the meshes towards the substrates. Eventually, the adhesion force from the substrates pulls the inks down in a close distance, resulting in pattern formation that is determined both by the properties of the inks and the size of the meshes. Screen printing is notable for its low fabrication cost and capability to print single or stacked layers onto variety of soft materials such as fabrics and plastic films. The ability of screen printing technique has been demonstrated majorly in the area of printing organic devices such as organic light-emitting diode (OLEDs) [112], organic field-effect transistor (OFETs) [113,114], thin film batteries [115–117], and organic solar cells [118,119]. In addition, it has been widely used to fabrication various flexible and stretchable electronic components, including antennas [120], metal conductors [121,122], and thin-film transistors [123–125]. Limitations of screen printing include limited selection of ink materials, short processing time influenced by solvent evaporation, and low printing resolution (>10 μm).

4.2.2. Inkjet Printing

Inkjet printing is considered as an additive manufacturing technique that is attractive for making electronic components on flexible substrates without using any photomask. Inks that contain either fully dissolved chemicals [126,127] or nanoparticles [128–131] can be deposited through inkjet nozzles, which are actuated through a number of mechanisms such as piezoelectricity and aerosol. Post sintering processing after inkjet printing using direct heating, microwave, laser, and pulsed light can enhance the performance of the printed patterns by converting individual nanoparticles into connected matrixes. Inkjet printing techniques have been used to fabricate various electronic devices. Passive components such as resistors [132–134], capacitors [135–137] and inductors [138] have been printed on polymer substrates with various functional inks. Active components such as thin film transistors [139–141] and LED [142–144] have also been fabricated using inkjet printing methods. Development of colloidal solution for proper ejection of droplets on a targeted area by keeping an acceptable quality of the printed circuits is challenging due to the influence of evaporation rate of the solvents and orientation of the active particles. Despite the advancement of both control electronics and nozzle technology in inkjet printing, its printing speed (at the scale of 10 $mm \cdot s^{-1}$) are still low as compared with screen printing methods, and its capability in printing complex structures such as serpentine and meander is still demanding further improvement. In addition, possibility of nozzle clogging and limited numbers of nozzles that can work simultaneously making inkjet printing methods more a rapid prototyping tool in labs rather than an acceptable mass fabrication method for industry. The spreading of the printed ink on target substrates and chaotic behavior of droplets during the time of flight further add to the issues of inkjet systems.

4.2.3. Transfer Printing

Transfer printing is an essential procedure to obtain flexible CMOS/MEMS devices. The target devices can be firstly fabricated on a donate substrate and then transferred to a receiving substrate using a viscoelastic stamp (usually a PDMS stamp) (Figure 4c). In this process, the adhesive strength is directly proportional to separation speed of the stamp from a surface. The effective separation speed between the stamp and the substrates is approximately 10 $cm \cdot s^{-1}$ or greater during a retrieval process, and is a few $mm \cdot s^{-1}$ or less for the printing process. Transfer printing technique has been extensively exploited to assemble diverse classes of materials (e.g., semiconductors, metals, carbon, and organic),

thereby providing an effective method to fabricate various devices ranging from simple light emitting diodes [145], transistors [146,147] and sensor elements to fully integrated circuits [148].

5. Applications of Flexible and Stretchable Skin Sensors

Mechanisms, materials and fabrication approaches mentioned above can be used to construct diverse skin sensors that offer broad applications in health monitoring, daily activity tracking, and rehabilitation. These skin sensors have been used to record biophysical signals such as biopotential, skin strain, temperature, and hydration. In addition, initial efforts have been made to conduct specific biomolecule analysis using body fluids (e.g., sweat and blood) through direct contact or transdermal sensing approaches.

5.1. Biopotential Measurement

Biopotential measurement using skin sensors represents one of the most important applications of skin sensors. Due to the capability to be mounted on different locations of human skin, electrodes based on stretchable conductive meshes typically made of copper and gold have been used to conduct electroencephalogram (EEG), electrooculogram (EOG), and electrocardiogram (ECG) measurements on body. Yeo et al. [149] have introduced a multifunctional epidermal electronic systems measuring electrophysiological based on skin-contacted metallic electrodes or meshes made of gold and copper, which can measure ECG, EMG, temperature and strain (Figure 5a). Due to close skin contact, the flexible and stretchable skin electrodes can directly contact with skin with a contact resistance at a scale of 35 kΩ, which is compared smaller than conventional dry electrodes (~40 kΩ). Non-contact biopotential sensing is also feasible. Jeong et al. have demonstrated capacitive electrodes that can measure biopotential signals without direct contact with skin [18] (Figure 5b). They have also presented another skin sensor that measures EMG signal induced by arm and wrist movement to control unman drone.

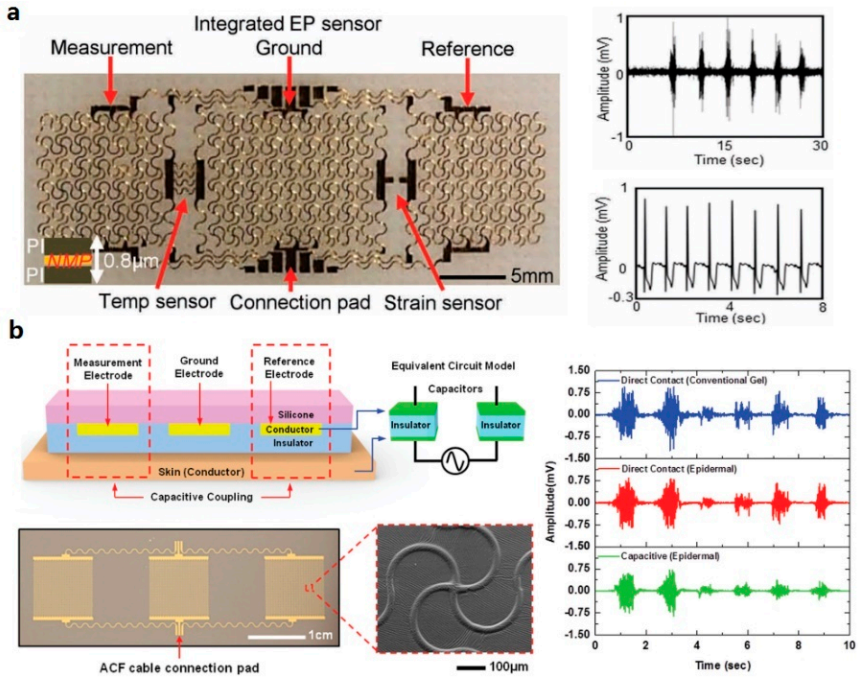

Figure 5. Examples of skin sensors for biopotential measurement: (**a**) biopotential measurement using skin-contacted metallic electrodes (Reprinted with permission from Ref. [91] Copyright 2013 John Wiley and Sons); and (**b**) an epidermal electronic system (EES) with a capacitive sensor for electrophysiological (EP) measurement (Reprinted with permission from Ref. [18] Copyright 2014 John Wiley and Sons).

5.2. Strain Sensing

Strain sensors can be directly attached on skin to measure strain induced by skin deformations caused by respiration, heartbeat, bending of body joints and muscle activities. Strain sensors can be fabricated by diverse materials and methods [17,150,151] with applications ranging from personalized health-monitoring [152,153] to human-machine interfaces [154,155] and soft robotics [156–158]. Park et al. [17] have achieved a stretchable graphene strain sensor using a layer-by-layer assembly method, in which stretchable yarns are repeatedly dip-coated with poly(vinyl alcohol) and graphene nanoplatelets bilayer. This strain sensor can be attached to throat and monitors the motions caused by speaking with maximum stretchability of ~100% (Figure 6a). Surface matrixes made of carbon nanotube and silicone rubber have been used to make strain sensors (Figure 6b). Carbon nanotubes were first coated onto a patterned polyimide film through air spraying, and were then transferred onto an Ecoflex film by casting uncured Ecoflex onto a polyimide film. The carbon nanotubes and Ecoflex form surface matrix that can be separated from the polyimide after the curing of the Ecoflex, resulting in conductive composite with high stretchability (~500%), linear temperature response ($R^2 = 1$) and fast time response (~332 ms) [150]. Majidi et al. [151] have developed thin-film curvature sensors composed of microfluidic channels filled with liquid metal (eGaIn) embedded in PDMS or Ecoflex substrates. The sensors can offer up to 1000% stretchability and measure both bending curvature and strain within the substrates with a gauge factor of 2 and a Young's modulus of 0.1~1 Mpa. Roh et al. [87] have realized a transparent and patchable strain sensor that is made of a sandwich-like stacked piezoresistive nanohybrid film of single-wall carbon nanotubes (SWCNTs) and a conductive elastomeric composite of polyurethane (PU)-poly(3,4-ethylenedioxythiophene) polystyrenesulfonate (PEDOT:PSS). This sensor can offer stretchability of up to 100% and optical transparency of 62%, which can detect small strains on human skin (Figure 6c).

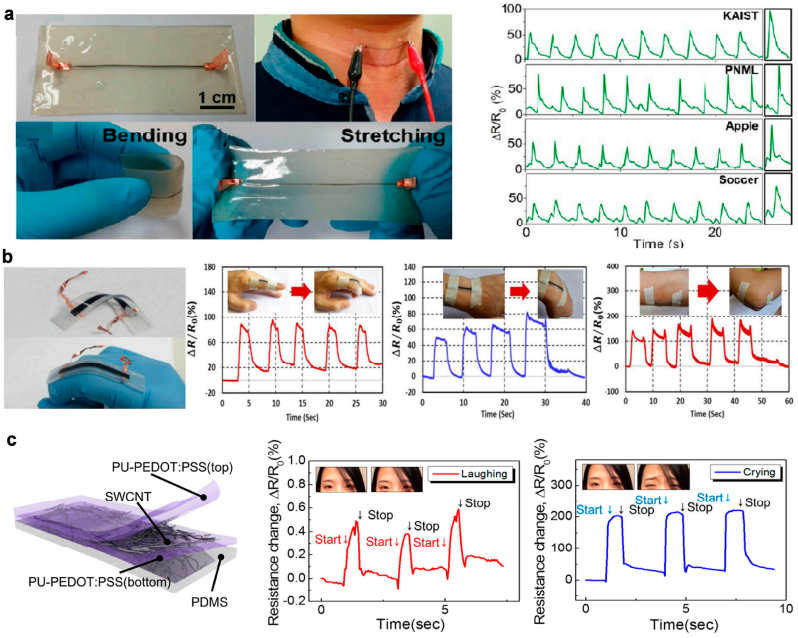

Figure 6. Examples of skin sensors for strain sensing: (**a**) graphene strain sensor embedded in an elastomeric patch that is bendable and stretchable, for detection of the motions of throat (Reprinted with permission from Ref. [17] Copyright 2015 American Chemical Society); (**b**) application of the CNT–Ecoflex nanocomposite based strain sensors to human motion detection (Reprinted with permission from Ref. [150] Copyright 2015 IOP Publishing); and (**c**) a transparent strain sensor consisting of three-layer stacked nanohybrid structure of PU-PEDOT:PSS/SWCNT/PU-PEDOT:PSS on a PDMS substrate (Reprinted with permission from Ref. [87] Copyright 2015 American Chemical Society).

5.3. Skin Temperature Monitoring

Temperature sensors are essential components for many health monitoring systems to determine both physiological and psychological conditions associated with cardiovascular health, cognitive state and malignancy. Skin temperature sensors can be conformably attached to skin surface, and, thus, can accurately measure body temperature with minimized influence from the environmental temperature. Examples of skin temperature sensors include arrays of meander metal wires that determine body temperature through measurement of spatial mapping, and temperature mapping devices based on PIN diodes made of silicon nanomembranes [159] (Figure 7a). To improve capability of long-term integration without disturbing the functions of skin, skin temperature sensors can be integrated with breathable substrates made of porous, semipermeable PU films (Figure 7b). The entire sensor is permeable to air and waterproof. It can realize continuous body temperature measuring for up to 24 h [28]. Organic materials can also be used to construct temperature sensors. Trung et al. [160] have realized a resistive and gated temperature sensor array purely by elastic organic materials with stretchability of ~70% and sensitivity of ~1.34% resistance change per degree Celsius. The sensing layer of this device can be formed by imbedding conductive and graphene oxide nanosheets into an elastomeric PU matrix (Figure 7c).

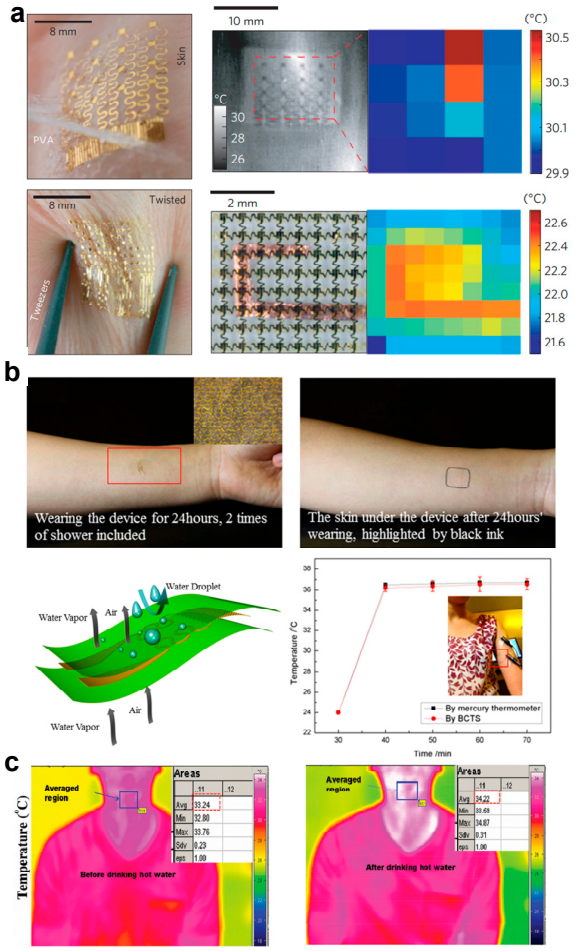

Figure 7. Examples of skin sensors for temepature measurement: (**a**) epidermal sensors that can monitor skin temperature using metallic and semiconductor sensors (Reprinted with permission from Ref. [159] Copyright 2013 Nature Publication Group); (**b**) breathable and stretchable temperature sensors (Reprinted with permission from Ref. [28] Copyright 2015 Nature Publication Group); and (**c**) transparent and stretchable temperature sensors (Reprinted with permission from Ref. [160] Copyright 2015 John Wiley and Sons).

5.4. Hydration Sensing

Accurately measurement of skin hydration levels is important for analyzing various diseases (e.g., dermatitis [161], psoriasis [162], eczema [163] and pruritus [164]) in the fields of dermatology and cosmetology, and evaluating factors (e.g., environmental [165], age [166], and hormone [167]) related to abnormal skin responses. In addition, hydration can also be used for assessing effectiveness of anti-aging treatment, moisturizing treatments and other medical therapies.

Skin hydration can be determined by measurements of electrical impedance, thermal conductivity, spectroscopic property, and mechanical characteristic in conventional approaches. The application of epidermal electronic techniques gives hydration sensing many advantages over traditional methods. Huang et al. have realized several types of epidermal hydration sensors based on detection of skin electrical impedance. The sensors consist of two electrodes connecting with a data acquisition system, which provides alternating electrical current at frequencies between 1 and 100 kHz. The skin electronic impedance can be reflected by resulting attenuation and phase shift of the electrical current. Devices capable of conducting differential monitoring [14] (Figure 8a), regional mapping [27] (Figure 8b), and wireless sensing [15] (Figure 8c) have been developed based on the impedance detection. In addition, hydration can also be assessed through measurements of skin thermal conductivity, which can be determined by time response of skin to constant thermal energy input [159].

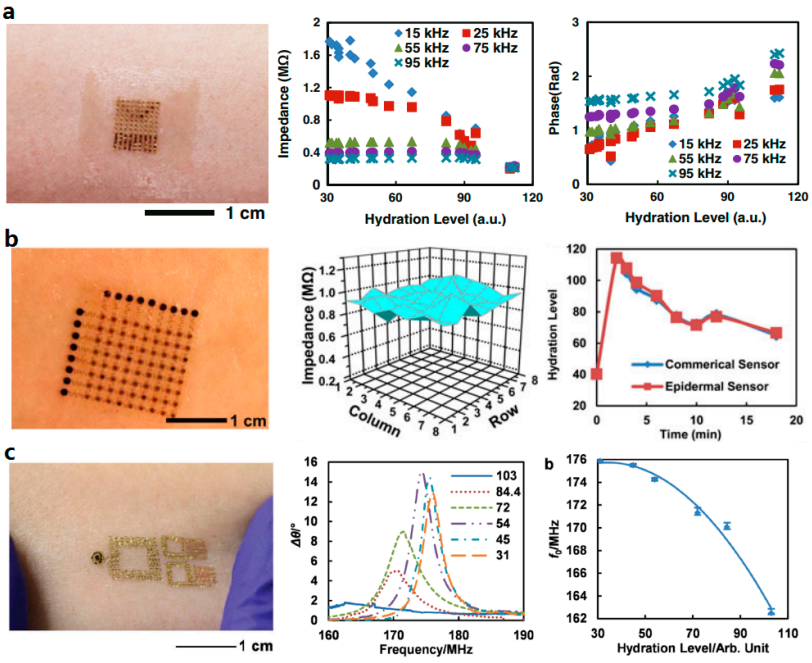

Figure 8. Examples of skin sensors used for hydration sensing: (**a**) epidermal sensor that can monitor biopotential on skin using metallic meshes (Reprinted with permission from Ref. [14] Copyright 2013 John Wiley and Sons); (**b**) hydration sensor that can conduct regional mapping based on the impedance detection (Reprinted with permission from Ref. [27] Copyright 2014 IEEE); and (**c**) hydration sensor capable of passive wireless detection (Reprinted with permission from Ref. [15] Copyright 2014 John Wiley and Sons).

5.5. Biomolecule Analysis

Flexible and stretchable skin sensors can be utilized for biomolecule analysis. Various biomolecules in sweat (e.g., sodium [12,168–170], potassium [12,169], ammonium [171,172], glucose [173], and lactate [12,174]) have been regarded as indicators for human physiological health. Huang et al. have explored materials and design strategies for integrating stretchable wireless sensors on porous sponge-like elastomeric substrates for epidermal analysis of biomolecules in sweat

(Figure 9a). The porous substrates allow sweat collection through capillary forces, without need for complex microfluidic handling systems. Colorimetric measurement is achieved in the same system by introducing indicator compounds into the substrates for sensing specific components (OH^-, H^+, Cu^+, and Fe^{2+}) in sweat [13]. Bandodkar et al. [175] have developed an epidermal tattoo-like sensor using a bluetooth enabled wearable transceiver for real-time monitoring of sodium in human perspiration with concentration range of 0.1–100 mM. This sensor can withstand strain caused by bending, stretching and poking (Figure 9b). Gao et al. [12] have designed a fully integrated sensor array for in situ perspiration analysis, which can simultaneously and selectively measure sweat metabolites (e.g., glucose and lactate) and electrolytes (e.g., sodium and potassium ions) as well as the skin temperature for sensor calibration (Figure 9c).

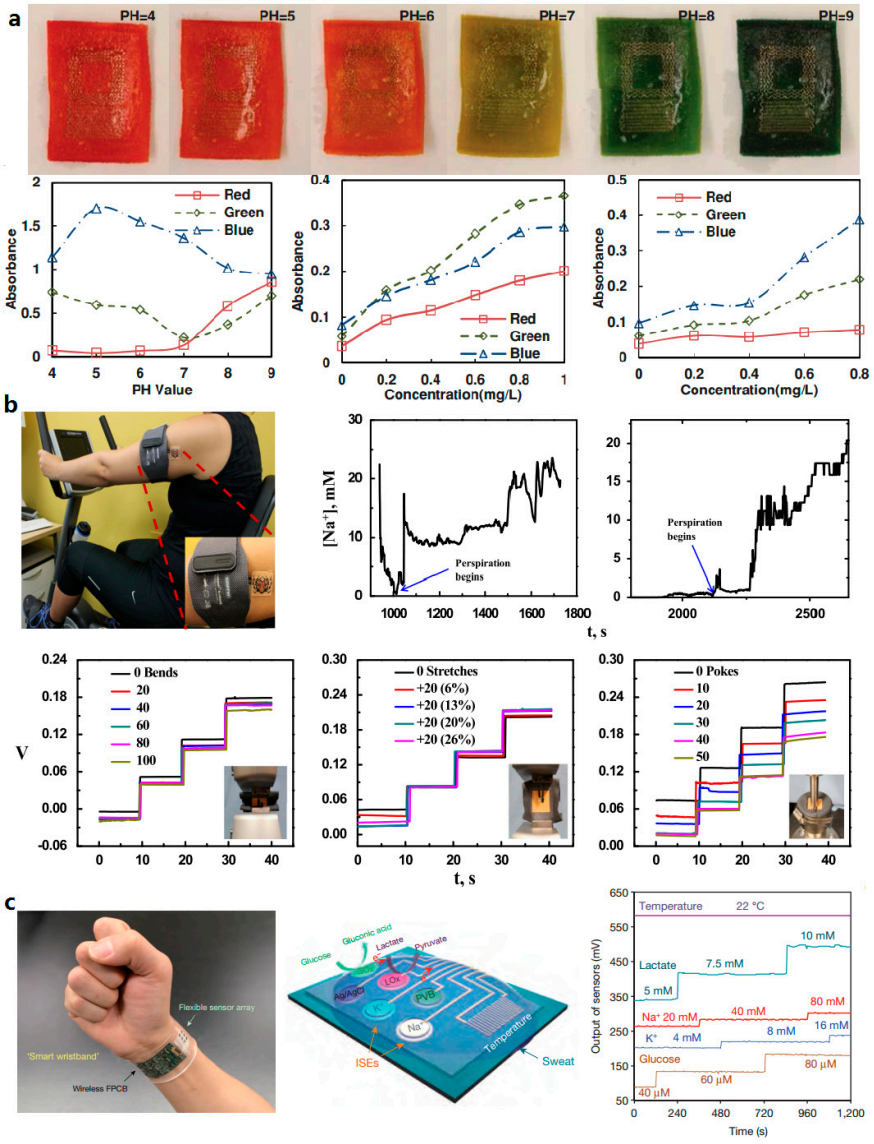

Figure 9. Examples of skin senosrs capable of conducting biomolecule analysis: (**a**) a skin sensor that can monitor biomolecules in sweat based on colorimetry approach (Reprinted with permission from Ref. [13] Copyright 2014 John Wiley and Sons); (**b**) a skin sensor that can monitor sodium in perspiration using electrochemical methods (Reprinted with permission from Ref. [175] Copyright 2014 Elsevier); and (**c**) a integrated system that can analyze multiple compositions in sweat simultaneously and selectively (Reprinted with permission from Ref. [12] Copyright 2016 Nature Publishing Group).

5.6. Other Sensing

Flexible and stretchable skin sensors also have other applications, including oximetry [21,176,177], pressure sensing [178,179] and wound healing monitoring [180,181]. For example, Yokota et al. [177] have developed optoelectronic skins integrated with OLED and organic photodetectors, which can measure the oxygen concentration of blood based on a photoplethysmogram (PPG) approach (Figure 10a). Choong et al. [182] have demonstrated a stretchable resistive pressure sensor within which the conductive electrode is built on the micro-pyramid PDMS arrays grafted with a PEDOT:PSS/PUD composite polymer. The sensor offers a pressure sensitivity of 10.3 kPa^{-1} when stretched by 40% (Figure 10b). Hattori et al. [180] have established an epidermal electronics system that can monitor cutaneous wound healing by recording time-dynamic temperature and thermal conductivity of skin. This system consists of metal traces with fractal and filamentary serpentine (FS) configurations, which can offer stretchability of ~30% (Figure 10c).

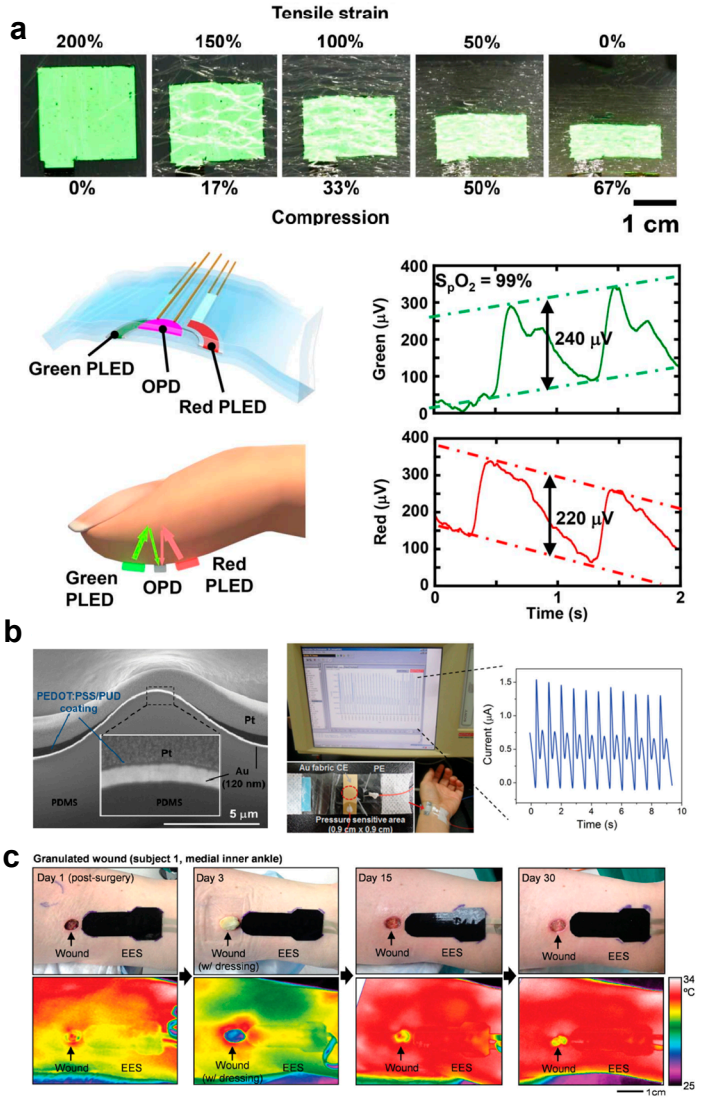

Figure 10. Skin sensors used for other sensing applications: (**a**) a skin sensor that can measure oxygen concentration of blood (Reprinted with permission from Ref [177] Copyright 2016 The Authors); (**b**) a stretchable resistive pressure sensor (Reprinted with permission from Ref [182] Copyright 2014 John Wiley and Sons); and (**c**) an epidermal electronics system that can monitor cutaneous wound healing (Reprinted with permission from Ref. [180] Copyright 2014 John Wiley and Sons).

6. Conclusions and Perspectives

This paper reviews the mechanisms, materials, fabrication techniques, and the representative applications of flexible and stretchable skin sensors. These sensors are constructed by various intrinsic soft materials or stretchable thin film structures with applications in biophysiological signal measurement and activity tracking, offering improved precision and effectiveness of body integration. Flexible and stretchable skin sensors can collect massive amount of data associated with personal biomedical information and life-style. These data can be used to assist more specific diagnosis and effective treatment of disease, and can potentially be used to reveal the underlying connection among biomedical information, environmental effects, and various diseases.

Despite the rapid progress in skin sensors, development of flexible and stretchable skin sensors has encountered several critical issues such as power supplies and system complexity. Firstly, most of the devices mentioned above focus on sensing functions of the stretchable electronic devices. However, power supply, signal conditioning, data communication, and data storage still largely rely on bulky instruments or integrated circuits based on rigid substrates. Some researches tackle the issues of power supplies with stretchable batteries [48,183], piezoelectric generators [184,185], solar cells [186,187], and wireless power harvesting [188], showing promising future in replacing current bulky power sources with components that mechanically and geometrically match stretchable electronic devices. While for signal conditioning and data communication, and data storage, these functions can be realized by integrating multiple commercial-off-the-shelf components connected by flexible and stretchable interconnects. These systems can be best represented by the work of Xu et al. [44] who realized a complex measurement system to detect biopotential, acceleration, temperature and achieve signal processing and wireless data communication with an operational amplifier-based circuit and a voltage control oscillator. The sweat sensing system [12] mentioned in the previous section has also demonstrated the possibility of integrating flexible circuits made of commercial components with stretchable skin sensor for precise analysis of sweat contents. These comprehensive systems will lead to capability to assess multiple biophysiological signals to improve accuracy in diagnosis and treatment. Discrete stretchable electronic components based purely on thin film materials and stretchable structures have been demonstrated as signal amplifiers [189], logic circuits [190,191], oscillators [192], and nonvolatile resistive memory [193,194]. However, a fully stretchable and integrated system has not yet been achieved due to the challenges in the fabrication of different functional components, interconnection of transfer printed components, and low electronic performance as compared to conventional devices based on rigid materials.

Furthermore, some fundamental knowledge of device mechanisms has not yet been well studied mechanically and electrically, and the interaction between the biological tissues and the flexible and stretchable skin sensors has not yet been well understood. For example, the electromagnetic properties of the stretchable structures such as serpentine, wavy, and out-of-plane buckling are largely unexplored, and the negative effects of the biological tissues to electromagnetic signal and optical signal have not yet been addressed to achieve optimized sensor performance. It can be expected that special properties offered by the sensor/skin interaction may be used to achieve more unique functions such as spontaneous actuation and transduction through skin motions, and the skin barrier functions may be overcome to allow analysis of biomolecules in blood and interstitial fluids using skin sensors. With more understanding of the fundamental knowledge of flexible and stretchable skin sensors, more sensing functions and powerful integrated systems may be developed based on the skin sensor platform, allowing revolutionary changes in the formats of continuous, long-term health monitoring devices to improve social health levels.

Acknowledgments: This work is supported by the National Natural Science Foundation of China under Grant No. 61604108 and the Natural Science Foundation of Tianjin under Grant No. 16JCYBJC40600.

Author Contributions: Xian Huang and Yicong Zhao conceived the article, constructed the graphs and wrote the paper. Xian Huang supervised the work.

Conflicts of Interest: The authors declare no conflict of interest.

References

1. Abdali-Mohammadi, F.; Bajalan, V.; Fathi, A. Toward a fault tolerant architecture for vital medical-based wearable computing. *J. Med. Syst.* **2015**, *39*, 149. [CrossRef] [PubMed]
2. Pantelopoulos, A.; Bourbakis, N.G. A survey on wearable sensor-based systems for health monitoring and prognosis. *IEEE Trans. Syst. Man Cybern. C* **2010**, *40*, 1–12. [CrossRef]
3. Yoo, J.; Yan, L.; Lee, S.; Kim, Y. A 5.2 mW self-configured wearable body sensor network controller and a 12 μW wirelessly powered sensor for a continuous health monitoring system. *IEEE J. Solid State Circuits* **2010**, *45*, 178–188. [CrossRef]
4. Evenson, K.R. Systematic review of the validity and reliability of consumer-wearable activity trackers. *Int. J. Behav. Nutr. Phys. Act.* **2015**, *12*, 159. [CrossRef] [PubMed]
5. Yang, C.-C.; Hsu, Y.L. A review of accelerometry-based wearable motion detectors for physical activity monitoring. *Sensors* **2010**, *10*, 7772–7788. [CrossRef] [PubMed]
6. Case, M.A.; Burwick, H.A.; Volpp, K.G.; Patel, M.S. Accuracy of smartphone applications and wearable devices for tracking physical activity data. *JAMA* **2015**, *313*, 625–626. [CrossRef] [PubMed]
7. Patel, S.; Park, H.; Bonato, P.; Chan, L.; Rodgers, M. A review of wearable sensors and systems with application in rehabilitation. *J. Neuroeng. Rehabil.* **2012**, *9*, 21. [CrossRef] [PubMed]
8. Chuah, H.W.; Rauschnabel, P.A.; Krey, N.; Bang, N.; Ramayah, T.; Lade, S. Wearable technologies: The role of usefulness and visibility in smartwatch adoption. *Comput. Hum. Behav.* **2016**, *65*, 276–284. [CrossRef]
9. Castillejo, P.; Martinez, J.F.; Rodriguez-Molina, J.; Cuerva, A. Integration of wearable devices in a wireless sensor network for an E-health application. *IEEE Wirel. Commun.* **2013**, *20*, 38–49. [CrossRef]
10. Ashley, E.A. The precision medicine initiative: A new national effort. *JAMA* **2015**, *313*, 2119–2120. [CrossRef] [PubMed]
11. Shah, S.H.; Arnett, D.; Houser, S.R.; Ginsburg, G.S.; Macrae, C.; Mital, S.; Loscalzo, J.; Hall, J.L. Opportunities for the cardiovascular community in the precision medicine initiative. *Circulation* **2016**, *133*, 226–231. [CrossRef] [PubMed]
12. Gao, W.; Emaminejad, S.; Nyein, H.Y.Y.; Challa, S.; Chen, K.; Peck, A.; Fahad, H.M.; Ota, H.; Shiraki, H.; Kiriya, D. Fully integrated wearable sensor arrays for multiplexed in situ perspiration analysis. *Nature* **2016**, *529*, 509–514. [CrossRef] [PubMed]
13. Huang, X.; Liu, Y.; Chen, K.; Shin, W.J.; Lu, C.J.; Kong, G.W.; Patnaik, D.; Lee, S.H.; Cortes, J.F.; Rogers, J.A. Stretchable, wireless sensors and functional substrates for epidermal characterization of sweat. *Small* **2014**, *10*, 3083–3090. [CrossRef] [PubMed]
14. Huang, X.; Yeo, W.H.; Liu, Y.; Rogers, J.A. Epidermal differential impedance sensor for conformal skin hydration monitoring. *Biointerphases* **2012**, *7*, 52. [CrossRef] [PubMed]
15. Huang, X.; Liu, Y.; Cheng, H.; Shin, W.J.; Fan, J.A.; Liu, Z.; Lu, C.J.; Kong, G.W.; Chen, K.; Patnaik, D. Materials and designs for wireless epidermal sensors of hydration and strain. *Adv. Funct. Mater.* **2014**, *24*, 3846–3854. [CrossRef]
16. Kim, J.; Salvatore, G.A.; Araki, H.; Chiarelli, A.M.; Xie, Z.; Banks, A.; Sheng, X.; Liu, Y.; Lee, J.W.; Jang, K.-I.; et al. Battery-free, stretchable optoelectronic systems for wireless optical characterization of the skin. *Sci. Adv.* **2016**, *2*, e1600418. [CrossRef] [PubMed]
17. Park, J.J.; Hyun, W.J.; Mun, S.C.; Park, Y.T.; Park, O.O. Highly stretchable and wearable graphene strain sensors with controllable sensitivity for human motion monitoring. *ACS Appl. Mater. Interfaces* **2015**, *7*, 6317–6324. [CrossRef] [PubMed]
18. Jeong, J.W.; Kim, M.K.; Cheng, H.; Yeo, W.H.; Huang, X.; Liu, Y.; Zhang, Y.; Huang, Y.; Rogers, J.A. Capacitive epidermal electronics for electrically safe, long-term electrophysiological measurements. *Adv. Healthc. Mater.* **2014**, *3*, 642–648. [CrossRef] [PubMed]

19. Maiti, R.; Gerhardt, L.-C.; Lee, Z.S.; Byers, R.A.; Woods, D.; Sanz-Herrera, J.A.; Franklin, S.E.; Lewis, R.; Matcher, S.J.; Carré, M.J. In vivo measurement of skin surface strain and sub-surface layer deformation induced by natural tissue stretching. *J. Mech. Behav. Biomed. Mater.* **2016**, *62*, 556–569. [CrossRef] [PubMed]
20. Kim, D.-H.; Lu, N.; Ma, R.; Kim, Y.-S.; Kim, R.-H.; Wang, S.; Wu, J.; Won, S.M.; Tao, H.; Islam, A.; et al. Epidermal electronics. *Science* **2011**, *333*, 838–843. [CrossRef] [PubMed]
21. Jang, K.-I.; Han, S.Y.; Xu, S.; Mathewson, K.E.; Zhang, Y.; Jeong, J.-W.; Kim, G.-T.; Webb, R.C.; Lee, J.W.; Dawidczyk, T.J.; et al. Rugged and breathable forms of stretchable electronics with adherent composite substrates for transcutaneous monitoring. *Nat. Commun.* **2014**, *5*, 4779. [CrossRef] [PubMed]
22. Yu, R.J.; Park, H.; Jin, S.W.; Hong, S.Y.; Lee, S.S.; Ha, J.S. Highly stretchable and sensitive strain sensors using fragmentized graphene foam. *Adv. Funct. Mater.* **2015**, *25*, 4228–4236.
23. Rogers, J.A.; Someya, T.; Huang, Y. Materials and mechanics for stretchable electronics. *Science* **2010**, *327*, 1603–1607. [CrossRef] [PubMed]
24. Song, J. Mechanics of stretchable electronics. *Curr. Opin. Solid State Mater. Sci.* **2015**, *19*, 160–170. [CrossRef]
25. Park, S.-I.; Ahn, J.-H.; Feng, X.; Wang, S.; Huang, Y.; Rogers, J.A. Theoretical and experimental studies of bending of inorganic electronic materials on plastic substrates. *Adv. Funct. Mater.* **2008**, *18*, 2673–2684. [CrossRef]
26. Kim, D.H.; Ahn, J.H.; Choi, W.M.; Kim, H.S.; Kim, T.H.; Song, J.; Huang, Y.Y.; Liu, Z.; Lu, C.; Rogers, J.A. Stretchable and foldable silicon integrated circuits. *Science* **2008**, *320*, 507–511. [CrossRef] [PubMed]
27. Huang, X.; Cheng, H.; Chen, K.; Zhang, Y.; Zhang, Y.; Liu, Y.; Zhu, C.; Ouyang, S.C.; Kong, G.W.; Yu, C. Epidermal impedance sensing sheets for precision hydration assessment and spatial mapping. *IEEE Trans. Biomed. Eng.* **2013**, *60*, 2848–2857. [CrossRef] [PubMed]
28. Chen, Y.; Lu, B.; Chen, Y.; Feng, X. Breathable and stretchable temperature sensors inspired by skin. *Sci. Rep.* **2015**, *5*, 11505. [CrossRef] [PubMed]
29. Kim, D.H.; Song, J.; Choi, W.M.; Kim, H.S.; Kim, R.H.; Liu, Z.; Huang, Y.Y.; Hwang, K.C.; Zhang, Y.W.; Rogers, J.A. Materials and noncoplanar mesh designs for integrated circuits with linear elastic responses to extreme mechanical deformations. *Proc. Natl. Acad. Sci. USA* **2008**, *105*, 18675–18680. [CrossRef] [PubMed]
30. Khang, D.Y.; Jiang, H.; Huang, Y.; Rogers, J.A. A stretchable form of single-crystal silicon for high-performance electronics on rubber substrates. *Science* **2006**, *311*, 208–212. [CrossRef] [PubMed]
31. Huang, Y.A.; Dong, W.; Huang, T.; Wang, Y.; Xiao, L.; Su, Y.; Yin, Z. Self-similar design for stretchable wireless LC strain sensors. *Sens. Actuators A Phys.* **2015**, *224*, 36–42. [CrossRef]
32. Lee, J.W.; Xu, R.; Lee, S.; Jang, K.I.; Yang, Y.; Banks, A.; Yu, K.J.; Kim, J.; Xu, S.; Ma, S. Soft, thin skin-mounted power management systems and their use in wireless thermography. *Proc. Natl. Acad. Sci. USA* **2016**, *113*, 201605720. [CrossRef] [PubMed]
33. Xu, S.; Yan, Z.; Jang, K.-I.; Huang, W.; Fu, H.; Kim, J.; Wei, Z.; Flavin, M.; McCracken, J.; Wang, R.; et al. Assembly of micro/nanomaterials into complex, three-dimensional architectures by compressive buckling. *Science* **2015**, *347*, 154–159. [CrossRef] [PubMed]
34. Khang, D.-Y.; Xiao, J.; Kocabas, C.; Maclaren, S.; Banks, T.; Jiang, H.; Huang, Y.Y.; Rogers, J.A. Molecular scale buckling mechanics in individual aligned single-wall carbon nanotubes on elastomeric substrates. *Nano Lett.* **2008**, *8*, 124–130. [CrossRef] [PubMed]
35. Xie, Y.; Liu, Y.; Zhao, Y.; Tsang, Y.; Lau, S.; Huang, H.; Chai, Y. Stretchable all-solid-state supercapacitor with wavy shaped polyaniline/graphene electrode. *J. Mater. Chem. A* **2014**, *2*, 9142–9149. [CrossRef]
36. Lee, G.B.; Sathi, S.G.; Kim, D.Y.; Jeong, K.U.; Nah, C. Wrinkled elastomers for the highly stretchable electrodes with excellent fatigue resistances. *Polym. Test.* **2016**, *53*, 329–337. [CrossRef]
37. Tuukkanen, S.; Hoikkanen, M.; Poikelispää, M.; Honkanen, M.; Vuorinen, T.; Kakkonen, M.; Vuorinen, J.; Lupo, D. Stretching of solution processed carbon nanotube and graphene nanocomposite films on rubber substrates. *Synth. Met.* **2014**, *191*, 28–35. [CrossRef]
38. Feng, X.; Yang, B.D.; Liu, Y.; Wang, Y.; Dagdeviren, C.; Liu, Z.; Carlson, A.; Li, J.; Huang, Y.; Rogers, J.A. Stretchable ferroelectric nanoribbons with wavy configurations on elastomeric substrates. *ACS Nano* **2011**, *5*, 3326–3332. [CrossRef] [PubMed]
39. Ryu, S.Y.; Xiao, J.; Park, W.I.; Son, K.S.; Huang, Y.Y.; Paik, U.; Rogers, J.A. Lateral buckling mechanics in silicon nanowires on elastomeric substrates. *Nano Lett.* **2009**, *9*, 3214–3219. [CrossRef] [PubMed]

40. Choi, W.M.; Song, J.; Khang, D.Y.; Jiang, H.; Huang, Y.Y.; Rogers, J.A. Biaxially stretchable "wavy" silicon nanomembranes. *Nano Lett.* **2007**, *7*, 1655–1663. [CrossRef] [PubMed]
41. Won, Y.; Kim, A.; Yang, W.; Jeong, S.; Moon, J. A highly stretchable, helical copper nanowire conductor exhibiting a stretchability of 700%. *NPG Asia Mater.* **2014**, *6*, e132. [CrossRef]
42. Gonzalez, M.; Axisa, F.; Bossuyt, F.; Hsu, Y.Y.; Vandevelde, B.; Vanfleteren, J. Design and performance of metal conductors for stretchable electronic circuits. *Circuit World* **2009**, *35*, 371–376. [CrossRef]
43. Xu, S.; Zhang, Y.; Cho, J.; Lee, J.; Huang, X.; Jia, L.; Fan, J.A.; Su, Y.; Su, J.; Zhang, H. Stretchable batteries with self-similar serpentine interconnects and integrated wireless recharging systems. *Nat. Commun.* **2013**, *4*, 66–78. [CrossRef] [PubMed]
44. Xu, S.; Zhang, Y.; Jia, L.; Mathewson, K.E.; Jang, K.I.; Kim, J.; Fu, H.; Huang, X.; Chava, P.; Wang, R. Soft microfluidic assemblies of sensors, circuits, and radios for the skin. *Science* **2014**, *344*, 70–74. [CrossRef] [PubMed]
45. Fan, J.A.; Yeo, W.H.; Su, Y.; Hattori, Y.; Lee, W.; Jung, S.Y.; Zhang, Y.; Liu, Z.; Cheng, H.; Falgout, L. Fractal design concepts for stretchable electronics. *Nat. Commun.* **2014**, *5*, 163–180. [CrossRef] [PubMed]
46. Zhu, S.; Huang, Y.; Li, T. Extremely compliant and highly stretchable patterned graphene. *Appl. Phys. Lett.* **2014**, *104*, 173103–173105. [CrossRef]
47. Fan, Z.; Zhang, Y.; Ma, Q.; Zhang, F.; Fu, H.; Hwang, K.C.; Huang, Y. A finite deformation model of planar serpentine interconnects for stretchable electronics. *Int. J. Solids Struct.* **2016**, *91*, 46–54. [CrossRef] [PubMed]
48. Zhang, Y.; Fu, H.; Su, Y.; Xu, S.; Cheng, H.; Fan, J.A.; Hwang, K.C.; Rogers, J.A.; Huang, Y. Mechanics of ultra-stretchable self-similar serpentine interconnects. *Acta Mater.* **2013**, *61*, 7816–7827. [CrossRef]
49. Kim, J.; Lee, M.; Shim, H.J.; Ghaffari, R.; Cho, H.R.; Son, D.; Jung, Y.H.; Soh, M.; Choi, C.; Jung, S. Stretchable silicon nanoribbon electronics for skin prosthesis. *Nat. Commun.* **2014**, *5*, 5747. [CrossRef] [PubMed]
50. Su, Y.; Wang, S.; Huang, Y.A.; Luan, H.; Dong, W.; Fan, J.A.; Yang, Q.; Rogers, J.A.; Huang, Y. Elasticity of fractal inspired interconnects. *Small* **2014**, *11*, 367–373. [CrossRef] [PubMed]
51. Wagner, S.; Bauer, S. Materials for stretchable electronics. *MRS Bull.* **2012**, *37*, 207–213. [CrossRef]
52. Kim, T.A.; Kim, H.S.; Sang, S.L.; Min, P. Single-walled carbon nanotube/silicone rubber composites for compliant electrodes. *Carbon* **2012**, *50*, 444–449. [CrossRef]
53. Choi, K.M.; Rogers, J.A. A photocurable poly (dimethylsiloxane) chemistry designed for soft lithographic molding and printing in the nanometer regime. *J. Am. Chem. Soc.* **2003**, *125*, 4060–4061. [CrossRef] [PubMed]
54. Puig-Lleixà, C.; Jiménez, C.L.; Alonso, J.; Bartrolí, J. Polyurethane–acrylate photocurable polymeric membrane for ion-sensitive field-effect transistor based urea biosensors. *Anal. Chim. Acta* **1999**, *389*, 179–188. [CrossRef]
55. Kokkinis, D.; Schaffner, M.; Studart, A.R. Multimaterial magnetically assisted 3D printing of composite materials. *Nat. Commun.* **2015**, *6*, 8643. [CrossRef] [PubMed]
56. Kramer, R.K.; Boley, J.W.; Stone, H.A.; Weaver, J.C.; Wood, R.J. Effect of microtextured surface topography on the wetting behavior of eutectic gallium-indium alloys. *Langmuir* **2014**, *30*, 533–539. [CrossRef] [PubMed]
57. Dickey, M.D.; Chiechi, R.C.; Larsen, R.J.; Weiss, E.A.; Weitz, D.A.; Whitesides, G.M. Eutectic gallium-indium (egain): A liquid metal alloy for the formation of stable structures in microchannels at room temperature. *Adv. Funct. Mater.* **2008**, *18*, 1097–1104. [CrossRef]
58. Liu, T.; Sen, P.; Kim, C.J. Characterization of nontoxic liquid-metal alloy galinstan for applications in microdevices. *J. Microelectromech. Syst.* **2012**, *21*, 443–450. [CrossRef]
59. Park, Y.-L.; Majidi, C.; Kramer, R.; Bérard, P.; Wood, R.J. Hyperelastic pressure sensing with a liquid-embedded elastomer. *J. Micromech. Microeng.* **2010**, *20*, 125029. [CrossRef]
60. Khan, M.R.; Hayes, G.J.; Zhang, S.; Dickey, M.D.; Lazzi, G. A pressure responsive fluidic microstrip open stub resonator using a liquid metal alloy. *IEEE Microw. Wirel. Compon. Lett.* **2012**, *22*, 577–579. [CrossRef]
61. Cheng, S.; Wu, Z. A microfluidic, reversibly stretchable, large-area wireless strain sensor. *Adv. Funct. Mater.* **2011**, *21*, 2282–2290. [CrossRef]
62. Cheng, S.; Rydberg, A.; Hjort, K.; Wu, Z. Liquid metal stretchable unbalanced loop antenna. *Appl. Phys. Lett.* **2009**, *94*, 144103. [CrossRef]
63. Jalali Mazlouman, S.; Jiang, X.J.; Mahanfar, A.; Menon, C.; Vaughan, R.G. A reconfigurable patch antenna using liquid metal embedded in a silicone substrate. *IEEE Trans. Antennas Propag.* **2011**, *59*, 4406–4412. [CrossRef]

64. Kim, H.-J.; Son, C.; Ziaie, B. A multiaxial stretchable interconnect using liquid-alloy-filled elastomeric microchannels. *Appl. Phys. Lett.* **2008**, *92*, 011904. [CrossRef]
65. Zhu, S.; So, J.-H.; Mays, R.; Desai, S.; Barnes, W.R.; Pourdeyhimi, B.; Dickey, M.D. Ultrastretchable fibers with metallic conductivity using a liquid metal alloy core. *Adv. Funct. Mater.* **2013**, *23*, 2308–2314. [CrossRef]
66. Vosgueritchian, M.; Lipomi, D.J.; Bao, Z. Highly conductive and transparent pedot: PSS films with a fluorosurfactant for stretchable and flexible transparent electrodes. *Adv. Funct. Mater.* **2012**, *22*, 421–428. [CrossRef]
67. Hyun, D.C.; Park, M.; Park, C.; Kim, B.; Xia, Y.; Hur, J.H.; Kim, J.M.; Park, J.J.; Jeong, U. Ordered zigzag stripes of polymer gel/metal nanoparticle composites for highly stretchable conductive electrodes. *Adv. Mater.* **2011**, *23*, 2946–2950. [CrossRef] [PubMed]
68. Joseph, N.; Janardhanan, C.; Sebastian, M.T. Electromagnetic interference shielding properties of butyl rubber-single walled carbon nanotube composites. *Compos. Sci. Technol.* **2014**, *101*, 139–144. [CrossRef]
69. Park, M.; Im, J.; Shin, M.; Min, Y.; Park, J.; Cho, H.; Park, S.; Shim, M.B.; Jeon, S.; Chung, D.Y.; et al. Highly stretchable electric circuits from a composite material of silver nanoparticles and elastomeric fibres. *Nat. Nanotechnol.* **2012**, *7*, 803–809. [CrossRef] [PubMed]
70. Shang, S.; Zeng, W.; Tao, X. High stretchable MWNTs/polyurethane conductive nanocomposites. *J. Mater. Chem.* **2011**, *21*, 7274–7280. [CrossRef]
71. Niu, Z.; Dong, H.; Zhu, B.; Li, J.; Hng, H.H.; Zhou, W.; Chen, X.; Xie, S. Highly stretchable, integrated supercapacitors based on single-walled carbon nanotube films with continuous reticulate architecture. *Adv. Mater.* **2013**, *25*, 1058–1064. [CrossRef] [PubMed]
72. Yamada, T.; Hayamizu, Y.; Yamamoto, Y.; Yomogida, Y.; Izadi-Najafabadi, A.; Futaba, D.N.; Hata, K. A stretchable carbon nanotube strain sensor for human-motion detection. *Nat. Nano* **2011**, *6*, 296–301. [CrossRef] [PubMed]
73. Lee, K.; Park, J.; Lee, M.-S.; Kim, J.; Hyun, B.G.; Kang, D.J.; Na, K.; Lee, C.Y.; Bien, F.; Park, J.-U. In-situ synthesis of carbon nanotube–graphite electronic devices and their integrations onto surfaces of live plants and insects. *Nano Lett.* **2014**, *14*, 2647–2654. [CrossRef] [PubMed]
74. Xu, F.; Lu, W.; Zhu, Y. Controlled 3D buckling of silicon nanowires for stretchable electronics. *ACS Nano* **2010**, *5*, 672–678. [CrossRef] [PubMed]
75. Xu, F.; Zhu, Y. Highly conductive and stretchable silver nanowire conductors. *Adv. Mater.* **2012**, *24*, 5117–5122. [CrossRef] [PubMed]
76. Kim, M.; Park, J.; Ji, S.; Shin, S.-H.; Kim, S.-Y.; Kim, Y.-C.; Kim, J.-Y.; Park, J.-U. Fully-integrated, bezel-less transistor arrays using reversibly foldable interconnects and stretchable origami substrates. *Nanoscale* **2016**, *8*, 9504–9510. [CrossRef] [PubMed]
77. Lee, M.-S.; Lee, K.; Kim, S.-Y.; Lee, H.; Park, J.; Choi, K.-H.; Kim, H.-K.; Kim, D.-G.; Lee, D.-Y.; Nam, S. High-performance, transparent, and stretchable electrodes using graphene–metal nanowire hybrid structures. *Nano Lett.* **2013**, *13*, 2814–2821. [CrossRef] [PubMed]
78. Akinwande, D.; Petrone, N.; Hone, J. Two-dimensional flexible nanoelectronics. *Nat. Commun.* **2014**, *5*, 5678. [CrossRef] [PubMed]
79. Roch, A.; Greifzu, M.; Talens, E.R.; Stepien, L.; Roch, T.; Hege, J.; Van Nong, N.; Schmiel, T.; Dani, I.; Leyens, C.; et al. Ambient effects on the electrical conductivity of carbon nanotubes. *Carbon* **2015**, *95*, 347–353. [CrossRef]
80. Bolotin, K.I.; Sikes, K.J.; Jiang, Z.; Klima, M.; Fudenberg, G.; Hone, J.; Kim, P.; Stormer, H.L. Ultrahigh electron mobility in suspended graphene. *Solid State Commun.* **2008**, *146*, 351–355. [CrossRef]
81. Lee, C.; Wei, X.; Kysar, J.W.; Hone, J. Measurement of the elastic properties and intrinsic strength of monolayer graphene. *Science* **2008**, *321*, 385–388. [CrossRef] [PubMed]
82. Lu, C.C.; Lin, Y.C.; Yeh, C.H.; Huang, J.C.; Chiu, P.W. High mobility flexible graphene field-effect transistors with self-healing gate dielectrics. *ACS Nano* **2012**, *6*, 4469–4474. [CrossRef] [PubMed]
83. Park, J.U.; Nam, S.W.; Lee, M.S.; Lieber, C.M. Synthesis of monolithic graphene–graphite integrated electronics. *Nat. Mater.* **2011**, *11*, 120–125. [CrossRef] [PubMed]
84. Sire, C.; Ardiaca, F.; Lepilliet, S.; Seo, J.W.T.; Hersam, M.C.; Dambrine, G.; Happy, H.; Derycke, V. Flexible gigahertz transistors derived from solution-based single-layer graphene. *Nano Lett.* **2012**, *12*, 1184. [CrossRef] [PubMed]

85. Lee, H.; Choi, T.K.; Lee, Y.B.; Cho, H.R.; Ghaffari, R.; Wang, L.; Choi, H.J.; Chung, T.D.; Lu, N.; Hyeon, T.; et al. A graphene-based electrochemical device with thermoresponsive microneedles for diabetes monitoring and therapy. *Nat. Nano* **2016**, *11*, 566–572. [CrossRef] [PubMed]
86. Kim, J.; Lee, M.-S.; Jeon, S.; Kim, M.; Kim, S.; Kim, K.; Bien, F.; Hong, S.Y.; Park, J.-U. Highly transparent and stretchable field-effect transistor sensors using graphene–nanowire hybrid nanostructures. *Adv. Mater.* **2015**, *27*, 3292–3297. [CrossRef] [PubMed]
87. Roh, E.; Hwang, B.U.; Kim, D.; Kim, B.Y.; Lee, N.E. Stretchable, transparent, ultrasensitive, and patchable strain sensor for human-machine interfaces comprising a nanohybrid of carbon nanotubes and conductive elastomers. *ACS Nano* **2015**, *9*, 6252–6261. [CrossRef] [PubMed]
88. Jariwala, D.; Sangwan, V.K.; Lauhon, L.J.; Marks, T.J.; Hersam, M.C. Emerging device applications for semiconducting two-dimensional transition metal dichalcogenides. *ACS Nano* **2014**, *8*, 1102–1120. [CrossRef] [PubMed]
89. Jang, H.; Park, Y.J.; Chen, X.; Das, T.; Kim, M.S.; Ahn, J.H. Graphene-based flexible and stretchable electronics. *Adv. Mater.* **2016**, *28*. [CrossRef] [PubMed]
90. Wang, C.; Takei, K.; Takahashi, T.; Javey, A. Carbon nanotube electronics–moving forward. *Chem. Soc. Rev.* **2013**, *42*, 2592–2609. [CrossRef] [PubMed]
91. Yeo, W.H.; Kim, Y.S.; Lee, J.; Ameen, A.; Shi, L.; Li, M.; Wang, S.; Ma, R.; Jin, S.H.; Kang, Z.; et al. Multifunctional epidermal electronics printed directly onto the skin. *Adv. Mater.* **2013**, *25*, 2773–2778. [CrossRef] [PubMed]
92. Karnaushenko, D.D.; Karnaushenko, D.; Makarov, D.; Schmidt, O.G. Compact helical antenna for smart implant applications. *NPG Asia Mater.* **2015**, *7*, e188. [CrossRef]
93. Sun, Y.; Kumar, V.; Adesida, I.; Rogers, J.A. Buckled and wavy ribbons of gaas for high-performance electronics on elastomeric substrates. *Adv. Mater.* **2006**, *18*, 2857–2862. [CrossRef]
94. Park, K.; Lee, D.-K.; Kim, B.-S.; Jeon, H.; Lee, N.-E.; Whang, D.; Lee, H.-J.; Kim, Y.J.; Ahn, J.-H. Stretchable, transparent zinc oxide thin film transistors. *Adv. Funct. Mater.* **2010**, *20*, 3577–3582. [CrossRef]
95. Wallentin, J.; Anttu, N.; Asoli, D.; Huffman, M.; Aberg, I.; Magnusson, M.H.; Siefer, G.; Fuss-Kailuweit, P.; Dimroth, F.; Witzigmann, B.; et al. InP nanowire array solar cells achieving 13.8% efficiency by exceeding the ray optics limit. *Science* **2013**, *339*, 1057–1060. [CrossRef] [PubMed]
96. Kim, R.-H.; Tao, H.; Kim, T.; Zhang, Y.; Kim, S.; Panilaitis, B.; Yang, M.; Kim, D.H.; Jung, Y.H.; Kim, B.H. Materials and designs for wirelessly powered implantable light-emitting systems. *Small* **2012**, *8*, 2812–2818. [CrossRef] [PubMed]
97. Savagatrup, S.; Printz, A.D.; Wu, H.; Rajan, K.M.; Sawyer, E.J.; Zaretski, A.V.; Bettinger, C.J.; Lipomi, D.J. Viability of stretchable poly(3-heptylthiophene) (P3HpT) for organic solar cells and field-effect transistors. *Synth. Met.* **2015**, *203*, 208–214. [CrossRef]
98. Mikhnenko, O.V.; Blom, P.W.M.; Nguyen, T.Q. Exciton diffusion in organic semiconductors. *Energy Environ. Sci.* **2015**, *8*, 1867–1888. [CrossRef]
99. Gwinner, M.C.; Pietro, R.D.; Vaynzof, Y.; Greenberg, K.J.; Ho, P.K.H.; Friend, R.H.; Sirringhaus, H. Doping of organic semiconductors using molybdenum trioxide: A quantitative time-dependent electrical and spectroscopic study. *Adv. Funct. Mater.* **2011**, *21*, 1432–1441. [CrossRef]
100. Kim, D.-H.; Rogers, J.A. Stretchable electronics: Materials strategies and devices. *Adv. Mater.* **2008**, *20*, 4887–4892. [CrossRef]
101. Sun, Y.; Choi, W.M.; Jiang, H.; Huang, Y.Y.; Rogers, J.A. Controlled buckling of semiconductor nanoribbons for stretchable electronics. *Nat. Nanotechnol.* **2006**, *1*, 201–207. [CrossRef] [PubMed]
102. Rojas, J.P.; Hussain, M.M. Flexible semi-transparent silicon (100) fabric with high-k/metal gate devices. *Phys. Status Solidi* **2013**, *7*, 187–191. [CrossRef]
103. Ghoneim, M.T.; Kutbee, A.; Nasseri, F.G.; Bersuker, G.; Hussain, M.M. Mechanical anomaly impact on metal-oxide-semiconductor capacitors on flexible silicon fabric. *Appl. Phys. Lett.* **2014**, *104*, 234104. [CrossRef]
104. Ghoneim, M.T.; Zidan, M.A.; Salama, K.N.; Hussain, M.M. Towards neuromorphic electronics: Memristors on foldable silicon fabric. *Microelectron. J.* **2014**, *45*, 1392–1395. [CrossRef]
105. Ghoneim, M.T.; Hussain, M.M. Study of harsh environment operation of flexible ferroelectric memory integrated with PZT and silicon fabric. *Appl. Phys. Lett.* **2015**, *107*, 495–502. [CrossRef]

106. Rojas, J.P.; Torres Sevilla, G.A.; Ghoneim, M.T.; Inayat, S.B.; Ahmed, S.M.; Hussain, A.M.; Hussain, M.M. Transformational silicon electronics. *ACS Nano* **2014**, *8*, 1468–1474. [CrossRef] [PubMed]
107. Ahmed, S.M.; Hussain, A.M.; Rojas, J.P.; Hussain, M.M. Solid state MEMS devices on flexible and semi-transparent silicon (100) platform. In Proceedings of the 2014 IEEE 27th International Conference on Micro Electro Mechanical Systems (MEMS), San Francisco, CA, USA, 26–30 January 2014; pp. 548–551.
108. Minemawari, H.; Yamada, T.; Matsui, H.; Tsutsumi, J.; Haas, S.; Chiba, R.; Kumai, R.; Hasegawa, T. Inkjet printing of single-crystal films. *Nature* **2011**, *475*, 364–367. [CrossRef] [PubMed]
109. Someya, T.S.T. Stretchable organic integrated circuits for large-area electronic skin surfaces. *MRS Bull.* **2012**, *37*, 236–245.
110. Faddoul, R.; Reverdy-Bruas, N.; Blayo, A. Formulation and screen printing of water based conductive flake silver pastes onto green ceramic tapes for electronic applications. *Mater. Sci. Eng. B* **2012**, *177*, 1053–1066. [CrossRef]
111. Kuo, H.P.; Yang, C.F.; Huang, A.N.; Wu, C.T.; Pan, W.C. Preparation of the working electrode of dye-sensitized solar cells: Effects of screen printing parameters. *J. Taiwan Inst. Chem. E* **2014**, *45*, 2340–2345. [CrossRef]
112. Jabbour, G.E.; Radspinner, R.; Peyghambarian, N. Screen printing for the fabrication of organic light-emitting devices. *IEEE J. Sel. Top. Quantum Electron.* **2001**, *7*, 769–773. [CrossRef]
113. Ren, X.; Pei, K.; Peng, B.; Zhang, Z.; Wang, Z.; Wang, X.; Chan, K. Low operating power and flexible active matrix organic transistor temperature sensors array. *Adv. Mater.* **2016**, *28*, 4832–4838. [CrossRef] [PubMed]
114. Rogers, J.A.; Bao, Z.; Raju, V.R. Nonphotolithographic fabrication of organic transistors with micron feature sizes. *Appl. Phys. Lett.* **1998**, *72*, 2716–2718. [CrossRef]
115. Xia, C.; Chen, F.; Liu, M. Reduced-temperature solid oxide fuel cells fabricated by screen-printing. *Electrochem. Solid State Lett.* **2001**, *4*, A52–A54. [CrossRef]
116. Kang, K.Y.; Lee, Y.G.; Dong, O.S.; Kim, J.C.; Kim, K.M. Performance improvements of pouch-type flexible thin-film lithium-ion batteries by modifying sequential screen-printing process. *Electrochim. Acta* **2014**, *138*, 294–301. [CrossRef]
117. Tehrani, Z.; Korochkina, T.; Govindarajan, S.; Thomas, D.J.; O'Mahony, J.; Kettle, J.; Claypole, T.C.; Gethin, D.T. Ultra-thin flexible screen printed rechargeable polymer battery for wearable electronic applications. *Org. Electron.* **2015**, *26*, 386–394. [CrossRef]
118. Krebs, F.C. Polymer solar cell modules prepared using roll-to-roll methods: Knife-over-edge coating, slot-die coating and screen printing. *Sol. Energy Mater. Sol. Cell* **2009**, *93*, 465–475. [CrossRef]
119. Shaheen, S.E.; Radspinner, R.; Peyghambarian, N.; Jabbour, G.E. Fabrication of bulk heterojunction plastic solar cells by screen printing. *Appl. Phys. Lett.* **2001**, *79*, 2996–2998. [CrossRef]
120. Song, L.; Myers, A.C.; Adams, J.J.; Zhu, Y. Stretchable and reversibly deformable radio frequency antennas based on silver nanowires. *ACS Appl. Mater. Interfaces* **2014**, *6*, 4248–4253. [CrossRef] [PubMed]
121. Yu, Y.; Yan, C.; Zheng, Z. Polymer-assisted metal deposition (PAMD): A full-solution strategy for flexible, stretchable, compressible, and wearable metal conductors. *Adv. Mater.* **2014**, *26*, 5508–5516. [CrossRef] [PubMed]
122. Guo, R.; Yu, Y.; Xie, Z.; Liu, X.; Zhou, X.; Gao, Y.; Liu, Z.; Zhou, F.; Yang, Y.; Zheng, Z. Matrix-assisted catalytic printing for the fabrication of multiscale, flexible, foldable, and stretchable metal conductors. *Adv. Mater.* **2014**, *25*, 3343–3350. [CrossRef] [PubMed]
123. Liang, J.; Tong, K.; Pei, Q. A water-based silver-nanowire screen-print ink for the fabrication of stretchable conductors and wearable thin-film transistors. *Adv. Mater.* **2016**, *28*, 5986–5996. [CrossRef] [PubMed]
124. Tong, K.; Liang, J.; Pei, Q. (Invited) intrinsically-stretchable, transparent thin film transistors. *ECS Trans.* **2016**, *75*, 205–212. [CrossRef]
125. Bao, Z.; Feng, Y.; Dodabalapur, A.; And, V.R.R.; Lovinger, A.J. High-performance plastic transistors fabricated by printing techniques. *Chem. Mater.* **1997**, *9*, 1299–1301. [CrossRef]
126. Lee, Y.; Choi, J.; Lee, K.J.; Stott, N.E.; Kim, D. Large-scale synthesis of copper nanoparticles by chemically controlled reduction for applications of inkjet-printed electronics. *Nanotechnology* **2008**, *19*, 415604. [CrossRef] [PubMed]
127. Li, D.; Sutton, D.; Burgess, A.; Graham, D.; Calvert, P.D. Conductive copper and nickel lines via reactive inkjet printing. *J. Mater. Chem.* **2009**, *19*, 3719–3724. [CrossRef]

128. Kic, P.; Liška, R. Formation of air-stable copper–silver core–shell nanoparticles for inkjet printing. *J. Mater. Chem.* **2009**, *19*, 3057–3062.
129. Ko, S.H.; Pan, H.; Grigoropoulos, C.P.; Luscombe, C.K.; Fréchet, J.M.J.; Poulikakos, D. All-inkjet-printed flexible electronics fabrication on a polymer substrate by low-temperature high-resolution selective laser sintering of metal nanoparticles. *Nanotechnology* **2007**, *18*, 345202. [CrossRef]
130. Tekin, E.; Smith, P.J.; Schubert, U.S. Inkjet printing as a deposition and patterning tool for polymers and inorganic particles. *Soft Matter* **2008**, *4*, 703–713. [CrossRef]
131. Crowley, K.; Morrin, A.; Hernandez, A.; O'Malley, E.; Whitten, P.G.; Wallace, G.G.; Smyth, M.R.; Killard, A.J. Fabrication of an ammonia gas sensor using inkjet-printed polyaniline nanoparticles. *Talanta* **2008**, *77*, 710–717. [CrossRef]
132. Kawase, T.; Sirringhaus, H.; Friend, R.H.; Shimoda, T. Inkjet printed via-hole interconnections and resistors for all-polymer transistor circuits. *Adv. Mater.* **2001**, *13*, 1601–1605. [CrossRef]
133. Jung, S.; Sou, A.; Gili, E.; Sirringhaus, H. Inkjet-printed resistors with a wide resistance range for printed read-only memory applications. *Org. Electron.* **2013**, *14*, 699–702. [CrossRef]
134. Kang, B.J.; Chang, K.L.; Oh, J.H. All-inkjet-printed electrical components and circuit fabrication on a plastic substrate. *Microelectron. Eng.* **2012**, *97*, 251–254. [CrossRef]
135. Cook, B.S.; Cooper, J.R.; Tentzeris, M.M. Multi-layer RF capacitors on flexible substrates utilizing inkjet printed dielectric polymers. *IEEE Microw. Wirel. Compon. Lett.* **2013**, *23*, 353–355. [CrossRef]
136. Riggs, B.; Elupula, R.; Grayson, S.; Chrisey, D. Photonic curing of aromatic thiol-ene click dielectric capacitors via inkjet printing. *J. Mater. Chem. A* **2014**, *2*, 17380–17386. [CrossRef]
137. Graddage, N.; Chu, T.Y.; Ding, H.; Py, C.; Dadvand, A.; Tao, Y. Inkjet printed thin and uniform dielectrics for capacitors and organic thin film transistors enabled by the coffee ring effect. *Org. Electron.* **2016**, *29*, 114–119. [CrossRef]
138. Lee, H.; Cook, B.S.; Murali, K.P.; Raj, M. Inkjet printed high-Q RF inductors on paper substrate with ferromagnetic nanomaterial. *IEEE Microw. Wirel. Compon. Lett.* **2016**, *26*, 1–3. [CrossRef]
139. Maccurdy, R.; Katzschmann, R.; Kim, Y.; Rus, D. Synthesis of ZnO nanoparticles to fabricate a mask-free thin-film transistor by inkjet printing. *J. Nanotechnol.* **2012**, *2012*.
140. Kawase, T.; Shimoda, T.; Newsome, C.; Sirringhaus, H.; Friend, R.H. Inkjet printing of polymer thin film transistors. *Thin Solid Films* **2003**, *438–439*, 279–287. [CrossRef]
141. Yan, H.; Chen, Z.; Zheng, Y.; Newman, C.; Quinn, J.R.; Dötz, F.; Kastler, M.; Facchetti, A. A high-mobility electron-transporting polymer for printed transistors. *Nature* **2009**, *457*, 679–686. [CrossRef] [PubMed]
142. O'Toole, M.; Shepherd, R.; Wallace, G.G.; Diamond, D. Inkjet printed led based pH chemical sensor for gas sensing. *Anal. Chim. Acta* **2009**, *652*, 308–314. [CrossRef] [PubMed]
143. Verma, A.; Zink, D.M.; Fléchon, C.; Carballo, J.L.; Flügge, H.; Navarro, J.M.; Baumann, T.; Volz, D. Efficient, inkjet-printed TADF-OLEDS with an ultra-soluble NHetPHOS complex. *Appl. Phys. A* **2016**, *122*, 1–5. [CrossRef]
144. Haverinen, H.M.; Myllyla, R.A.; Jabbour, G.E. Inkjet printed RGB quantum dot-hybrid LED. *J. Disp. Technol.* **2010**, *6*, 87–89. [CrossRef]
145. Park, S.I.; Xiong, Y.; Kim, R.H.; Elvikis, P.; Meitl, M.; Kim, D.H.; Wu, J.; Yoon, J.; Yu, C.J.; Liu, Z. Printed assemblies of inorganic light-emitting diodes for deformable and semitransparent displays. *Science* **2010**, *325*, 977–981. [CrossRef] [PubMed]
146. Ahn, J.H.; Kim, H.S.; Lee, K.J.; Jeon, S.; Kang, S.J.; Sun, Y.; Nuzzo, R.G.; Rogers, J.A. Heterogeneous three-dimensional electronics by use of printed semiconductor nanomaterials. *Science* **2006**, *314*, 1754–1757. [CrossRef] [PubMed]
147. Lee, K.J.; Ahn, H.; Motala, M.J.; Nuzzo, R.G.; Menard, E.; Rogers, J.A. Fabrication of microstructured silicon (μs-Si) from a bulk Si wafer and its use in the printing of high-performance thin-film transistors on plastic substrates. *J. Micromech. Microeng.* **2010**, *20*, 75018–75025. [CrossRef]
148. Cao, Q.; Kim, H.S.; Pimparkar, N.; Kulkarni, J.P.; Wang, C.; Shim, M.; Roy, K.; Alam, M.A.; Rogers, J.A. Medium-scale carbon nanotube thin-film integrated circuits on flexible plastic substrates. *Nature* **2008**, *454*, 495–500. [CrossRef] [PubMed]
149. Jeong, J.W.; Yeo, W.H.; Akhtar, A.; Norton, J.J.; Kwack, Y.J.; Li, S.; Jung, S.Y.; Su, Y.; Lee, W.; Xia, J. Materials and optimized designs for human-machine interfaces via epidermal electronics. *Adv. Mater.* **2013**, *25*, 6839–6846. [CrossRef] [PubMed]

150. Amjadi, M.; Yoon, Y.J.; Park, I. Ultra-stretchable and skin-mountable strain sensors using carbon nanotubes-ecoflex nanocomposites. *Nanotechnology* **2015**, *26*, 9–21. [CrossRef] [PubMed]
151. Majidi, C.; Kramer, R.; Wood, R.J. A non-differential elastomer curvature sensor for softer-than-skin electronics. *Smart Mater. Struct.* **2011**, *20*, 1487–1490. [CrossRef]
152. Zhang, J.; Liu, J.; Zhuang, R.; Mäder, E.; Heinrich, G.; Gao, S. Single MWNT-glass fiber as strain sensor and switch. *Adv. Mater.* **2011**, *23*, 3392–3397. [CrossRef] [PubMed]
153. Kang, I.; Schulz, M.J.; Kim, J.H.; Shanov, V.; Shi, D. A carbon nanotube strain sensor for structural health monitoring. *Smart Mater. Struct.* **2006**, *15*, 737–748. [CrossRef]
154. Muth, J.T.; Vogt, D.M.; Truby, R.L.; Mengüç, Y.; Kolesky, D.B.; Wood, R.J.; Lewis, J.A. Embedded 3D printing of strain sensors within highly stretchable elastomers. *Adv. Mater.* **2014**, *26*, 6307–6312. [CrossRef] [PubMed]
155. Yan, C.; Wang, J.; Kang, W.; Cui, M.; Wang, X.; Foo, C.Y.; Chee, K.J.; Lee, P.S. Highly stretchable piezoresistive graphene-nanocellulose nanopaper for strain sensors. *Adv. Mater.* **2014**, *26*, 2022–2027. [CrossRef] [PubMed]
156. Mcevoy, M.A.; Correll, N. Materials science. Materials that couple sensing, actuation, computation, and communication. *Science* **2015**, *347*. [CrossRef] [PubMed]
157. Majidi, C. Soft robotics: A perspective—Current trends and prospects for the future. *Soft Robot.* **2014**, *1*, 5–11. [CrossRef]
158. Kang, D.; Pikhitsa, P.V.; Choi, Y.W.; Lee, C.; Shin, S.S.; Piao, L.; Park, B.; Suh, K.Y.; Kim, T.I.; Choi, M. Ultrasensitive mechanical crack-based sensor inspired by the spider sensory system. *Nature* **2014**, *516*, 222–226. [CrossRef] [PubMed]
159. Webb, R.C.; Bonifas, A.P.; Behnaz, A.; Zhang, Y.; Yu, K.J.; Cheng, H.; Shi, M.; Bian, Z.; Liu, Z.; Kim, Y.S. Ultrathin conformal devices for precise and continuous thermal characterization of human skin. *Nat. Mater.* **2013**, *12*, 938–944. [CrossRef] [PubMed]
160. Trung, T.Q.; Ramasundaram, S.; Hwang, B.U.; Lee, N.E. An all-elastomeric transparent and stretchable temperature sensor for body-attachable wearable electronics. *Adv. Mater.* **2016**, *28*, 502–509. [CrossRef] [PubMed]
161. Sator, P.G.; Schmidt, J.B.; Hönigsmann, H. Comparison of epidermal hydration and skin surface lipids in healthy individuals and in patients with atopic dermatitis. *J. Am. Acad. Dermatol.* **2003**, *48*, 352–358. [CrossRef] [PubMed]
162. Kim, S.D.; Huh, C.H.; Seo, K.I.; Suh, D.H.; Youn, J.I. Evaluation of skin surface hydration in korean psoriasis patients: A possible factor influencing psoriasis. *Clin. Exp. Dermatol.* **2002**, *27*, 147–152. [CrossRef] [PubMed]
163. Berents, T.L.; Carlsen, K.C.L.; Mowinckel, P.; Skjerven, H.O.; Kvenshagen, B.; Rolfsjord, L.B.; Bradley, M.; Lieden, A.; Carlsen, K.; Gaustad, P. Skin barrier function and staphylococcus aureus colonization in vestibulum nasi and fauces in healthy infants and infants with eczema: A population-based cohort study. *PLoS ONE* **2015**, *10*, e0130145. [CrossRef] [PubMed]
164. Morton, C.A.; Lafferty, M.; Hau, C.; Henderson, I.; Jones, M.; Lowe, J.G. Pruritus and skin hydration during dialysis. *Nephrol. Dial. Transplant.* **1996**, *11*, 2031–2036. [CrossRef] [PubMed]
165. Cravello, B.; Ferri, A. Relationships between skin properties and environmental parameters. *Skin Res. Technol.* **2008**, *14*, 180–186. [CrossRef] [PubMed]
166. Woo, C.J.; Hyo, K.S.; Hun, H.C.; Chan, P.K.; Woong, Y.S. The influences of skin visco-elasticity, hydration level and aging on the formation of wrinkles: A comprehensive and objective approach. *Skin Res. Technol.* **2013**, *19*, e349–e355.
167. Sator, P.G.; Schmidt, J.B.; Rabe, T.; Zouboulis, C.C. Skin aging and sex hormones in women—Clinical perspectives for intervention by hormone replacement therapy. *Exp. Dermatol.* **2004**, *13* (Suppl. 4), 36–40. [CrossRef] [PubMed]
168. Parrilla, M.; Ferré, J.; Guinovart, T.; Andrade, F.J. Wearable potentiometric sensors based on commercial carbon fibres for monitoring sodium in sweat. *Electroanal* **2016**, *28*, 1267–1275. [CrossRef]
169. Parrilla, M.; Cánovas, R.; Jeerapan, I.; Andrade, F.J.; Wang, J. A textile-based stretchable multi-ion potentiometric sensor. *Adv. Healthc. Mater.* **2016**, *5*, 996–1001. [CrossRef] [PubMed]
170. Cazalé, A.; Sant, W.; Ginot, F.; Launay, J.C.; Savourey, G.; Revol-Cavalier, F.; Lagarde, J.M.; Heinry, D.; Launay, J.; Temple-Boyer, P. Physiological stress monitoring using sodium ion potentiometric microsensors for sweat analysis. *Sens. Actuators B Chem.* **2015**, *225*, 1211–1219. [CrossRef]

171. Guinovart, T.; Bandodkar, A.J.; Windmiller, J.R.; Andrade, F.J.; Wang, J. A potentiometric tattoo sensor for monitoring ammonium in sweat. *Analyst* **2013**, *138*, 7031–7038. [CrossRef] [PubMed]
172. Bandodkar, A.J.; Jeerapan, I.; You, J.M.; Nuñezflores, R.; Wang, J. Highly stretchable fully-printed cnt-based electrochemical sensors and biofuel cells: Combining intrinsic and design-induced stretchability. *Nano Lett.* **2016**, *16*, 721–727. [CrossRef] [PubMed]
173. Kudo, H.; Sawada, T.; Kazawa, E.; Yoshida, H.; Iwasaki, Y.; Mitsubayashi, K. A flexible and wearable glucose sensor based on functional polymers with soft-mems techniques. *Biosens. Bioelectron.* **2006**, *22*, 558–562. [CrossRef] [PubMed]
174. Labroo, P.; Cui, Y. Flexible graphene bio-nanosensor for lactate. *Biosens. Bioelectron.* **2013**, *41*, 852–856. [CrossRef] [PubMed]
175. Bandodkar, A.J.; Molinnus, D.; Mirza, O.; Guinovart, T.; Windmiller, J.R.; Valdés-Ramírez, G.; Andrade, F.J.; Schöning, M.J.; Wang, J. Epidermal tattoo potentiometric sodium sensors with wireless signal transduction for continuous non-invasive sweat monitoring. *Biosens. Bioelectron.* **2013**, *54*, 603–609. [CrossRef] [PubMed]
176. Lochner, C.M.; Khan, Y.; Pierre, A.; Arias, A.C. All-organic optoelectronic sensor for pulse oximetry. *Nat. Commun.* **2014**, *5*, 5745. [CrossRef] [PubMed]
177. Yokota, T.; Zalar, P.; Kaltenbrunner, M.; Jinno, H.; Matsuhisa, N.; Kitanosako, H.; Tachibana, Y.; Yukita, W.; Koizumi, M.; Someya, T. Ultraflexible organic photonic skin. *Sci. Adv.* **2016**, *2*, e1501856. [CrossRef] [PubMed]
178. Gong, S.; Schwalb, W.; Wang, Y.; Chen, Y.; Tang, Y.; Si, J.; Shirinzadeh, B.; Cheng, W. A wearable and highly sensitive pressure sensor with ultrathin gold nanowires. *Nat. Commun.* **2013**, *5*, 163–180. [CrossRef] [PubMed]
179. Vandeparre, H.; Watson, D.; Lacour, S.P. Extremely robust and conformable capacitive pressure sensors based on flexible polyurethane foams and stretchable metallization. *Appl. Phys. Lett.* **2013**, *103*, 204103. [CrossRef]
180. Hattori, Y.; Falgout, L.; Lee, W.; Jung, S.Y.; Poon, E.; Lee, J.W.; Na, I.; Geisler, A.; Sadhwani, D.; Zhang, Y. Multifunctional skin-like electronics for quantitative, clinical monitoring of cutaneous wound healing. *Adv. Healthc. Mater.* **2014**, *3*, 1597–1607. [CrossRef] [PubMed]
181. Lin, S.; Yuk, H.; Zhang, T.; Parada, G.A.; Koo, H.; Yu, C.; Zhao, X. Stretchable hydrogel electronics and devices. *Adv. Mater.* **2015**, *53*, 735–741. [CrossRef] [PubMed]
182. Choong, C.L.; Shim, M.B.; Lee, B.S.; Jeon, S.; Ko, D.S.; Kang, T.H.; Bae, J.; Lee, S.H.; Byun, K.E.; Im, J. Highly stretchable resistive pressure sensors using a conductive elastomeric composite on a micropyramid array. *Adv. Mater.* **2014**, *26*, 3451–3458. [CrossRef] [PubMed]
183. Gaikwad, A.M.; Zamarayeva, A.M.; Rousseau, J.; Chu, H.; Derin, I.; Steingart, D.A. Highly stretchable alkaline batteries based on an embedded conductive fabric. *Adv. Mater.* **2012**, *24*, 5071–5076. [CrossRef] [PubMed]
184. Lee, J.-H.; Lee, K.Y.; Gupta, M.K.; Kim, T.Y.; Lee, D.-Y.; Oh, J.; Ryu, C.; Yoo, W.J.; Kang, C.-Y.; Yoon, S.-J.; et al. Highly stretchable piezoelectric-pyroelectric hybrid nanogenerator. *Adv. Mater.* **2014**, *26*, 765–769. [CrossRef] [PubMed]
185. Duan, Y.; Huang, Y.; Yin, Z.; Bu, N.; Dong, W. Non-wrinkled, highly stretchable piezoelectric devices by electrohydrodynamic direct-writing. *Nanoscale* **2014**, *6*, 3289–3295. [CrossRef] [PubMed]
186. Lipomi, D.J.; Tee, B.C.K.; Vosgueritchian, M.; Bao, Z. Stretchable organic solar cells. *Adv. Mater.* **2011**, *23*, 1771–1775. [CrossRef] [PubMed]
187. Li, G.; Zhu, R.; Yang, Y. Polymer solar cells. *Nat. Photon.* **2012**, *6*, 153–161. [CrossRef]
188. Huang, X.; Liu, Y.; Kong, G.W.; Seo, J.H.; Ma, Y.; Jang, K.-I.; Fan, J.A.; Mao, S.; Chen, Q.; Li, D.; et al. Epidermal radio frequency electronics for wireless power transfer. *Microsyst. Nanoeng.* **2016**, *2*, 16052. [CrossRef]
189. Münzenrieder, N.; Cantarella, G.; Vogt, C.; Petti, L.; Büthe, L.; Salvatore, G.A.; Fang, Y.; Andri, R.; Lam, Y.; Libanori, R.; et al. Stretchable and conformable oxide thin-film electronics. *Adv. Electron. Mater.* **2015**, *1*, 1400038. [CrossRef]
190. Zhang, X.; Zhao, J.; Dou, J.; Tange, M.; Xu, W.; Mo, L.; Xie, J.; Xu, W.; Ma, C.; Okazaki, T.; et al. Flexible CMOS-like circuits based on printed p-type and n-type carbon nanotube thin-film transistors. *Small* **2016**, *12*, 5066–5073. [CrossRef] [PubMed]

191. Xu, W.; Liu, Z.; Zhao, J.; Xu, W.; Gu, W.; Zhang, X.; Qian, L.; Cui, Z. Flexible logic circuits based on top-gate thin film transistors with printed semiconductor carbon nanotubes and top electrodes. *Nanoscale* **2014**, *6*, 14891–14897. [CrossRef] [PubMed]
192. Kim, B.; Park, J.; Geier, M.L.; Hersam, M.C.; Dodabalapur, A. Voltage-controlled ring oscillators based on inkjet printed carbon nanotubes and zinc tin oxide. *ACS Appl. Mater. Interfaces* **2015**, *7*, 12009–12014. [CrossRef] [PubMed]
193. Cheng, C.H.; Yeh, F.S.; Chin, A. Low-power high-performance non-volatile memory on a flexible substrate with excellent endurance. *Adv. Mater.* **2011**, *23*, 902–905. [CrossRef] [PubMed]
194. Ji, Y.; Cho, B.; Song, S.; Kim, T.W.; Choe, M.; Kahng, Y.H.; Lee, T. Stable switching characteristics of organic nonvolatile memory on a bent flexible substrate. *Adv. Mater.* **2010**, *22*, 3071–3075. [CrossRef] [PubMed]